DESIGN OF A 750 KV BUSHING

A DISSERTATION

Submitted in partial fulfilment of the
requirement for the award of the degree
of
MASTER OF ENGINEERING
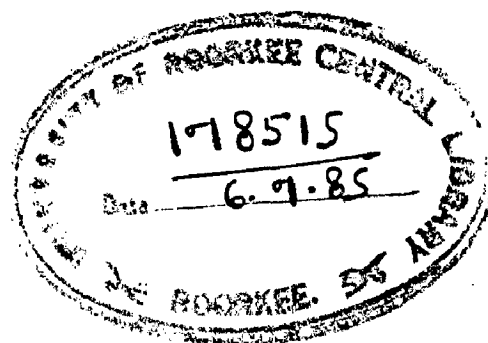in
ELECTRICAL ENGINEERING
(Power System Engineering)

By

KRISHNA KUMAR JAISWAL

DEPARTMENT OF ELECTRICAL ENGINEERING
UNIVERSITY OF ROORKEE
ROORKEE-247667 (India)

April, 1985
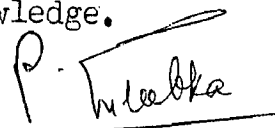
(i)

CANDIDATE'S DECLARATION

I hereby certify that the work which is being presented in the dissertation entitled DESIGN OF A 750 KV BUSHING in partial fulfilment of the requirements for the degree of MASTER OF ENGINEERING IN ELECTRICAL ENGINEERING (Power System Engineering) submitted in the Department of Electrical Engineering, University of Roorkee, Roorkee is an authentic record of my own work carried out during a period of eight months from August, 1984 to April 1985 under the supervision of Dr. P.Suleebka, Reader, Electrical Engineering Department, University of Roorkee, Roorkee.

The matter embodied in this dissertation has not been submitted for the award of any other degree or diploma.

Krishna Kumar Jaiswal
(KRISHNA KUMAR JAISWAL)

This is to certify that the above statement made by the candidate is correct to the best of my knowledge.

ROORKEE

(Dr.P.SULEEBKA)
Reader (H.V.)

DATE: APRIL 6 ,1985.

Electrical Engineering Dept.,
University of Roorkee,
Roorkee.

ACKNOWLEDGEMENT

ABSTRACT

A survey of literature is done to get the possible detailed information about bushings, but it does not give any existing design in 750 KV range. Therefore it is decided to design 750 KV bushing from very basic considerations. Here we have designed 750 KV, 2000A (current rating to conform with IEC standards) outdoor-immersed bushing.

Three types of bushing are designed, viz., Oil Impregnated Paper (OIP), Synthetic Resin Bonded Paper (SRBP) and Oil-filled with metallic cyclindrical equipotentials. Among them, the OIP bushing is found to be most suitable for this range. A computer programme is also developed for this design which is also helpful in calculating thermal performance of the bushing. The final size of the bushing is proportionately matching with existing designs for other voltage levels.

CONTENTS

REFERENCES

BIBLIOGRAPHY

APPENDICES

       A   - Testing of Bushings

       B   - Operating Condition of Bushing and
            information to be furnished when ordering
            or markings.

       C   - Detection of Discharges

       D,E and F - Computer Programmes.

0.0 INTRODUCTION

A bushing is a structure carrying one or several conductors through a partition such as a wall or tank, etc. and insulating it or them therefrom, including the means of attachment (flange or other fixing device) to the partition. The conductor may be an integral part of the bushing or be drawn into a central tube contained in the bushing. Bushings have to provide electrical insulation of the conductor for the working voltage and for the various over-voltages which occur in service and also have to provide mechanical support against various mechanical forces. It is usually composed of an outer porcelain body and at higher voltages additional insulation in the form of oil and molded paper is used within this porcelain.

In the first high -voltage transformers wood or porcelain bushings were used for bringing out the terminals, but as the voltages increased, the wood bushings were lined with a very heavy glass tube. Then long tubes of treated paper were adopted and these were finally replaced by the condenser type of bushings. General electric Company (USA) have also developed a special type of oil-filled bushing with insulating barriers.

The bushings are broadly classified into two types:

0.1 NON-CONDENSER BUSHINGS: [Fig.1]

In its simplest form a bushing would be a simple cyclinder of insulating material: porcelain glass, synthetic resin bonded paper (SRBP), cast resin, polythene, hard rubber etc. with radial and axial clearances to suit the electric strengths of the insulating material and the surrounding media respectively. The voltage is not at all evenly distributed through the wall thickness or along the length of the insulation and as voltages increase the dimensions required become so large that really high-voltage bushings of this form are not a practicable proposition.

0.2 CONDENSER BUSHINGS : [Fig. 2]

This difficulty is overcome by the condenser bushings in which the wall thickness is divided up into a number of capacitors by concentric conducting cylinders. Other methods of grading are used, i.e. a series of concentric barriers of higher dielectric constant than oil suitably arranged in a porcelain shell filled with oil. However the condenser construction gives much more compact designs than any other construction. Condenser bushings are broadly classified in following categories:

1. Current carrying rod.
2. Flange.
3. Insulating body.

Fig. 1:— Non Condenser Bushing.

Equipotential
Cylinders.
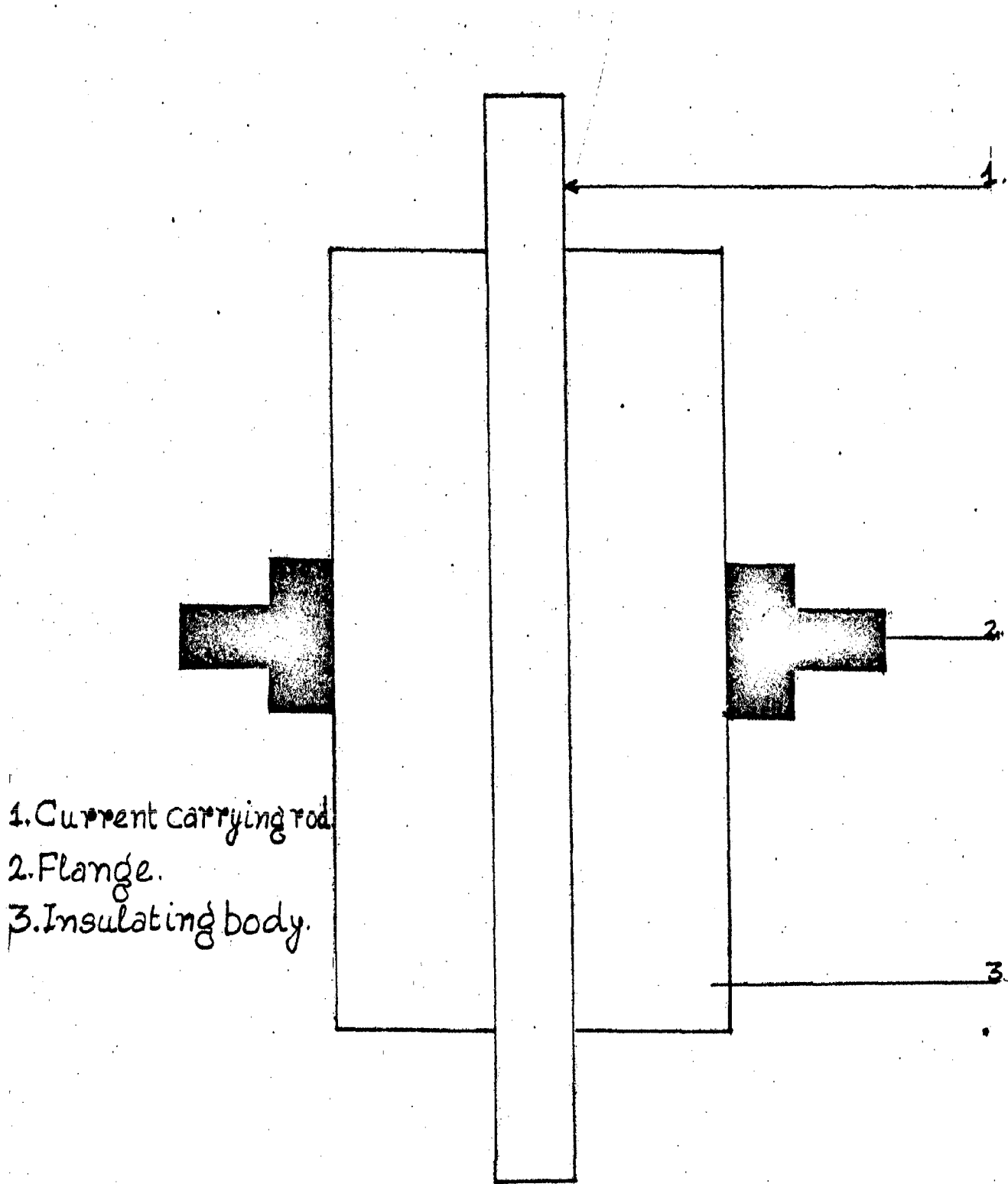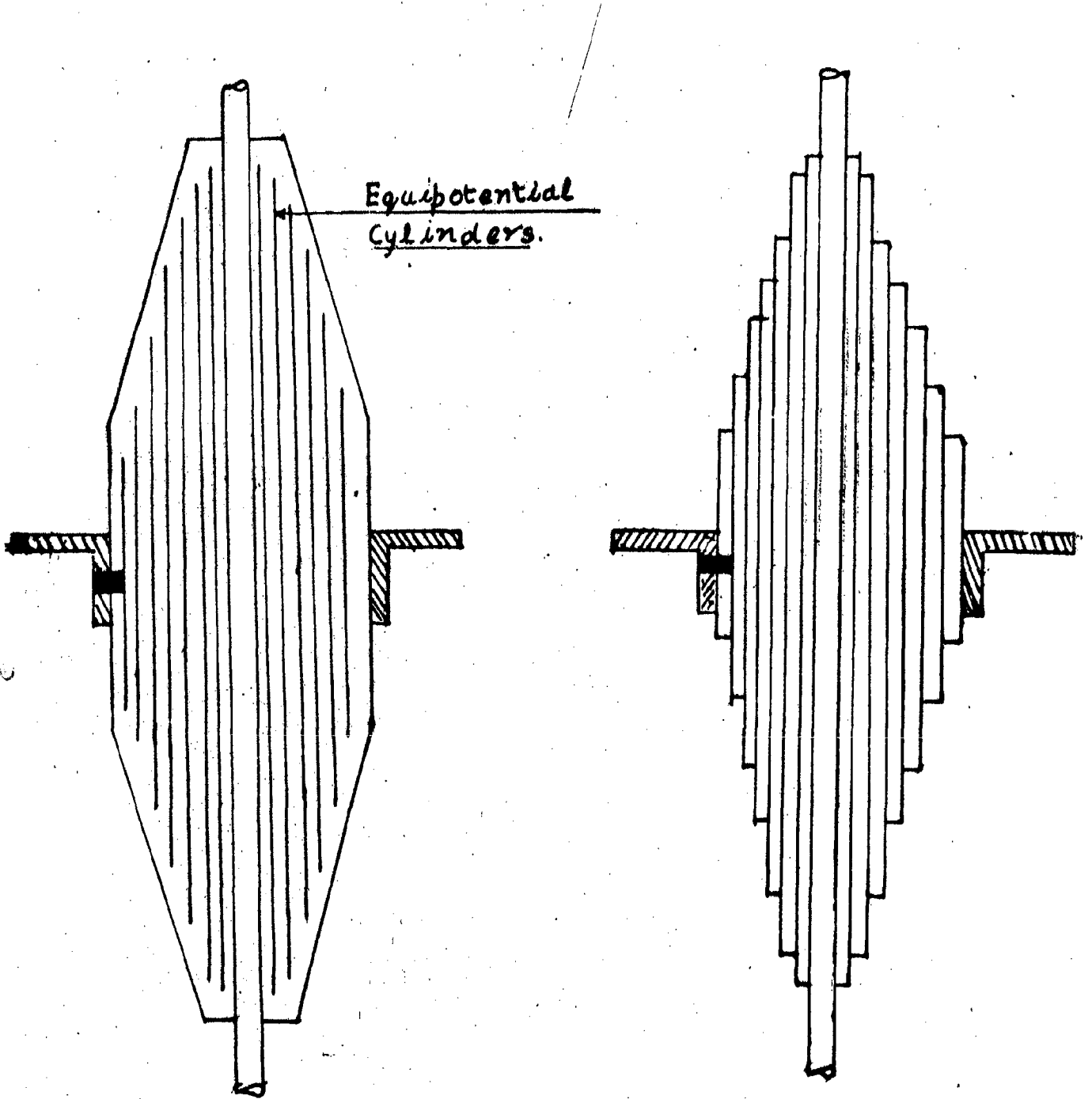
Fig. 2. Bushings with capacitance grading

0.2.1 Oil Impregnated paper bushings :

An oil impregnated paper type bushing employs the untreated paper which is wound directly on a metallic central tube. Conducting layers of metal foil are inserted at predetermined diameters. The whole winding operation is done under heat and pressure to ensure homogenous winding. Normally wherever full width of paper could not be used, paper tapes can be spirally wound. The wound conderser core is subsequently vacaum dried and vaccum impregnated with oil. The drying and impregnating process should be carefully done to produce partial discharge free bushings. To assess the dryness of the condenser either the analysis of exhaust from the vaccum pump for moisture detection can be used or the properties of condenser like capacitance and loss angle can be measured. However, great care should also be exercised when impregnating the condenser core with oil. The oil used should be processed to remove the moisture content and dissolved gases. The impregnated core is then assembled with porcelain and other metallic fittings to form a complete bushing.

0.2.2 Synthetic Resin Bonded Paper Busing :

SRBP bushings are manufactured with the help of resin coated paper wound on a metallic tube with predetermined insertion of conducting layers. Here again a uniform

winding is done under heat and pressure. After the
winding the core is machined to the desired dimensions
before the bushing is assembled. The core at lower end
of the bushing is given a special weather proof coating
since there is no porcelain employed.

Comparison of OIP and SRBP Busings:

In OIP bushings the partial discharge level is
comparatively lower than SRBP bushings by virtue of careful
winding, drying and impregnating processes. SRBP bushings
will have voids between layers which will lead to inter-
nal discharges. Repeated impulses at high voltage level
can cause the internal discharges to re-appear mainly at
the layer edges. Due to the lower dielectric constant of
the air in the voids compared with that of the active
dielectric materials, the stress in these voids are
increased considerably leading to breakdown. The design
should take care to ensure uniformity of stress at all
points.

Full width of resin coated paper is not available
for extra high voltages. Hence for extra high voltages
SRBP bushings cannot be manufactured. For OIP bushings
even though the full width paper may not be available the
paper tapes can be used. So for ehv range, generally
OIP bushings are used.

0.2.3 Oil-Filled Bushings : [Fig.3]

This type of bushing consists of porcelain shell,
generally in the form of petticoat insulations through
which extends a copper tube. The space between the porcelain shell
shell and this copper tube is filled with oil, an oil
glass gauge being provided at the upper end for ins-
pection purposes. The conductor consists of a flexible
conductor that is located inside of the copper tube. A
series of concentric barriers of higher dielectric
constant than oil suitablly arranged in the porcelain
shell filled with oil. The porcelain shell is generally
made in two sections held together by means of a metal
sleeve which forms the section of the bushing that comes
in contact with the transformer tank.
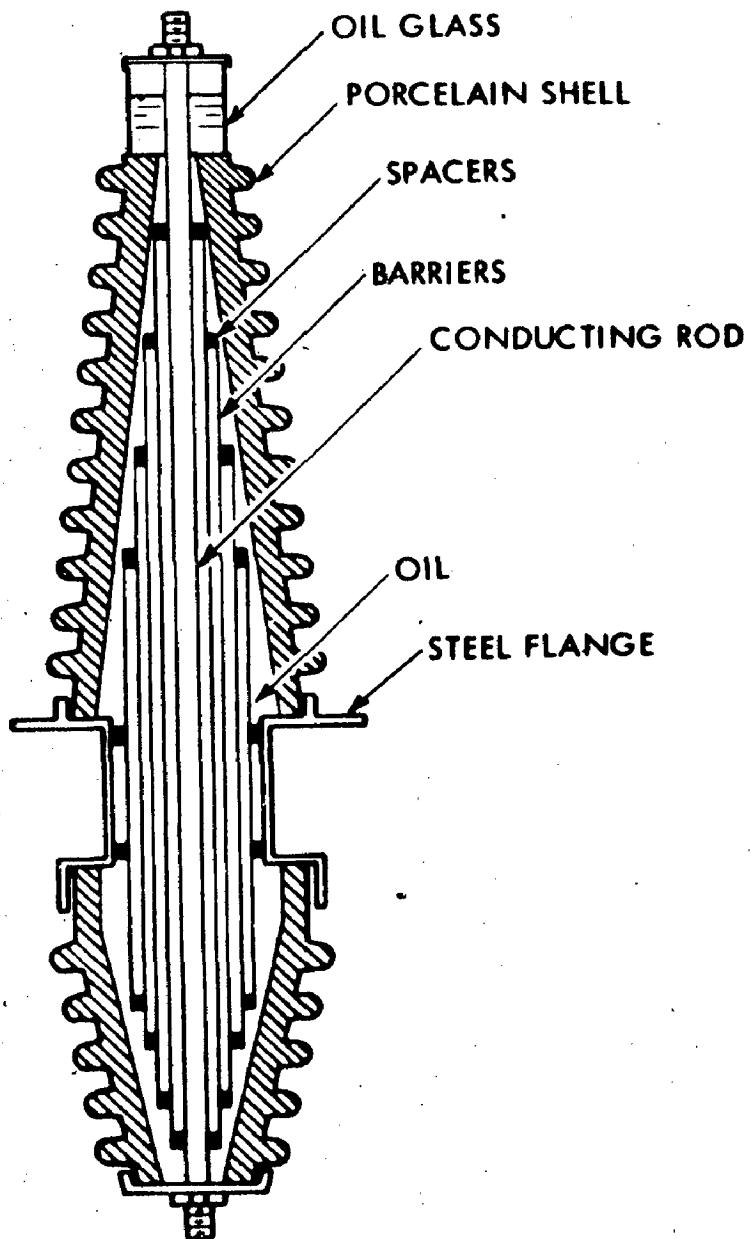
Fig. 3 :-   Oil-filled bushing.

1.0 PROBLEMS ASSOCIATED WITH BUSHINGS :

1. Thermal Stability

2. Internal Discharges

3. Flashover and breakdown along laminae

4. Flashover of external insulation

5. Manufacture of large insulating bodies

6. Atmospheric pollution effects and moisture influence.

1.1 THERMAL STABILITY :

The theory of thermal breakdown states the following: at elevated operating temperatures, stable thermal equilibrium is assured only when a maximum value of sustained voltage, the characterstic of the particular bushing, is not exeeeded. The thermal performance of a bushing mainly depends on the quality of the dielectric, its ambient temperature, and the manner in which it is internally cooled.

With S.R.B.P. bushings the power factor at the maximum oil temperature reached by transformers about $80^{\circ}C$ is high enough to produce considerable dielectric losses and with large bushings there may be a danger of thermal instability. On bushings of low current ratings (upto say 600 A at 132 KV) the conductor losses are of the order of the dielectric losses but with higher current ratings the conductor losses are much more than dielectric losses.

In O.I.P. busings, dielectric losses are lesser in comparison to S.R.B.P. bushings. In large O.I.P. bushings for heavy current e.g. a 400 KV, 1600 A-transformer bushing, the conductor losses are several times the dielectric losses and it is usual practice to consider the dissipation of conductor losses in the design of high current ehv bushings.

Three possible failure modes due to thermal degratation can be indentified as potential problems in a less conservative design or application practice. All three of these could result in dielectric breakdown of the bushing.

(i) Thermal degradation of insulation resulting in an accelerating increase in dissipation factor.

(ii) Oil expansion causing internal pressure to build up to a level sufficient to blow out a gasket.

(iii) Gasket hardening from high temperature resulting in an ultimate loss of seal.

Although failure by any of these three modes would not necessarily occur at the time of an excessive overload, the detoriation effects would be cumulative. Unless preventive maintenance detected the changing condition of the bushing, the consequence could range from an unplanned outage for bushing replacement to serious domage to the transformer.

1.2 INTERNAL DISCHARGES IN BUSHINGS :

A satisfactory bushing is one which has been so designed that it will withstand without breakdown during its life the maximum working voltage plus any overvoltages it may be subjected to either in service or during testing.

The working voltage requirement demands the consideration of long-term breakdown which in the cases of both S.R.B.P. or O.I.P. is usually due to internal discharges though by somewhat different mechanisms.

S.R.B.P.Bushings: -

S.R.B.P. for high voltage bushings consists of discrete layers of paper bonded together with thin films of resin. It, therefore, contains a considerable amount of air uniformly distributed between the fibres of paper. When the voltage on a bushing is raised a value is reached at which the minute pockets of air in the regions of highest stress begin to discharge. These regions are at the ends of equipotential layers where the stress reaches several times the radial stress between the layers, depending upon the spacing between the layers. In addition the hazards of bushing manufacture may result in circumferential cracking due to the stresses set up by the differential between radial and circumferential shrinkage or to weak resin bonding due to incorrect winding condition. In the

discrete voids formed in this way the electric stress
is increased considerably due to the low dielectric
constant of the air compared with the rest of the
material. The magnitude of a discharge which occurs in a
void is limited by the surface resistivity within the void.
Thus discharges in voids in contact with metallic layers or co-
nductors are more intense and more damaging.

The effects of discharges occuring in s.r.b.p. are
well known though the exact mechanism by which the material
is destroyed locally could be any of the following. The
effects may be chemical, due to the formation of oxides of
— —nitrogen-or-ozone in the discharge on the cellulose or
they may be due to temperature or ionic bombardment. Some
discharges produce a carbonless erosion which gradually
extends in a radial direction until a layer is punctured.
This effect occurs mainly at the ends of equipotential
layers. In other cases the discharge extends axially from
the end of a layer forming a carbonized tree-like path
and some examples have occured of a discharge in a localized
void progressing radially through the wall of the insulation.
All the above forms of the discharges are progressive
and ultimately result in a breakdown over a long period.
Final breakdown may occur due to residual over-stressed
material being unable to withstand a surge or becoming
thermally unstable. Breakdowns due to discharges at

working voltage thus occur from periods of several weeks upward to several years. Over voltages which occur in service are usually surges due to switching or lightening. In normal design of condenser bushings, the breakdown is axial from the ends of the layers, it occurs in a very short time (a few micro seconds) and is no doubt the result of breakdown of the air in the paper. The complete breakdown of a bushing may be complex e.g. the axial breakdown of the material over some distance may so increase the radial stress locally that it punctures radially, again by breakdown of the air in the paper. Localized circumferential cracking or poor bonding may complicate the breakdown by providing an air path of low dielectric strength in which the breakdown is initiated.

Purely localized radial breakdown can occur at high stresses, due to local weakness such as local mechanical puncture due to a small foreign body being wound in.

During testing of bushings high-power frequency voltages are applied and instantaneous breakdown along the laminations may occur by the same mechanisms as for surges. There is also the possibility of local high-intensity discharges producing a thermal breakdown in times ranging from seconds to hours.

Oil impregnated paper bushings:

There are no gaseous inclusions in oil-impregnated paper bushings which have been properly processed and adequately impregnated. Internal discharges do not occur therefore at the same stress levels as for s.r.b.p. The generation of gas bubbles in oil in the presence of fibrous material containing small amounts of water takes place. The stress levels required are much higher than the working stresses in bushings, even allowing for the large increase in stress at the edges of equipotential layers, but under surge or test conditions at high power frequency voltages such high stresses are attained.

Repeated impulse voltages giving stresses of the order of 250 to 300 KV/cm (surface stress on a layer- not edge stress which will be very much higher) produce an effect of dryness at the edges of the layers as if the oil had been driven away from the edges. Many impulses are required to produce an effect detectable by a progressive reduction in discharge inception and extinction voltages. It appears to be reversible and after some hours the discharge inception voltage is restored to a high level.

It follows from this that an impulse imposed on a bushing already subjected to a power-frequency stress can initiate a discharge which will persist at the power frequency stress level. Such discharges are of relatively

low intensity and are no doubt similar to those
which occur in oil-impregnated paper which is
inadequately impregnated. Very low progressive
deterioration occurs in which polymerization of the
oil into 'cable wax' can also occur, as in cables.

At high power-frequency stresses discharges
occur at the edges of the layers which can propogate
rapidly in oil-impregnated paper. The discharge is
presumably initiated in the $s_{am}e$ manner as with
repeated impulses but the high repetition rate results
in rapid propogation, ranging from just perceptible
spikes of carbonization at the ends of the layers to
more extensive tree-marking following paths along the
laminations. At high enough stresses the destructive
effect of the discharges is sufficient to extend
radially through several layers of paper and local
punctures occur leading rapidly to complete breakdown.

There are two aspects of discharges inside bushings.
Firstly, as we see from the above discussion, internal
discharges attacks the dielectric and thus weakens the
bushing electrically, secondly, the presence of such
discharges may prove an obstacle to the detection of
partial discharges inside a transformer.

1.3 FLASHOVER AND BREAKDOWN ALONG LAMINAE:

The greatest wekness of every laminated insulating material is its low electric strength in the direction of lamination, which is usually only a fraction of the strength perpendicular to the layer. This applies to both resin bonded and oil impregnated paper. Flashover from the embedded edge of a capacitor layer along the paper laminae represents a very serious problem, especially in a low point of a transformer bushing. As curve 1 of Fig. 4 shows that the rise in breakdown voltage along the laminae is no where near proportional to the flashover distance. Thus to test EHV bushings, the bottom part would have to be disproportionately long. In the resin bonded paper bushings the length can be shortened by simple means, in addition to which the longitudional stress is improved. This is done by machining away the resin bonded paper down to the capacitor layers, so that the edges of the latter are situated at the paper-oil interface. The effect is shown in curve (2) of Fig. 4.

1.4 FLASHOVER OF EXTERNAL INSULATION :

In Fig. (5) values of the flashover voltages measured in air along condenser bushings are plotted against the flashover distance. Where-as the impulse withstand voltage increases in proportion to the distance, the electric strength with respect to the power
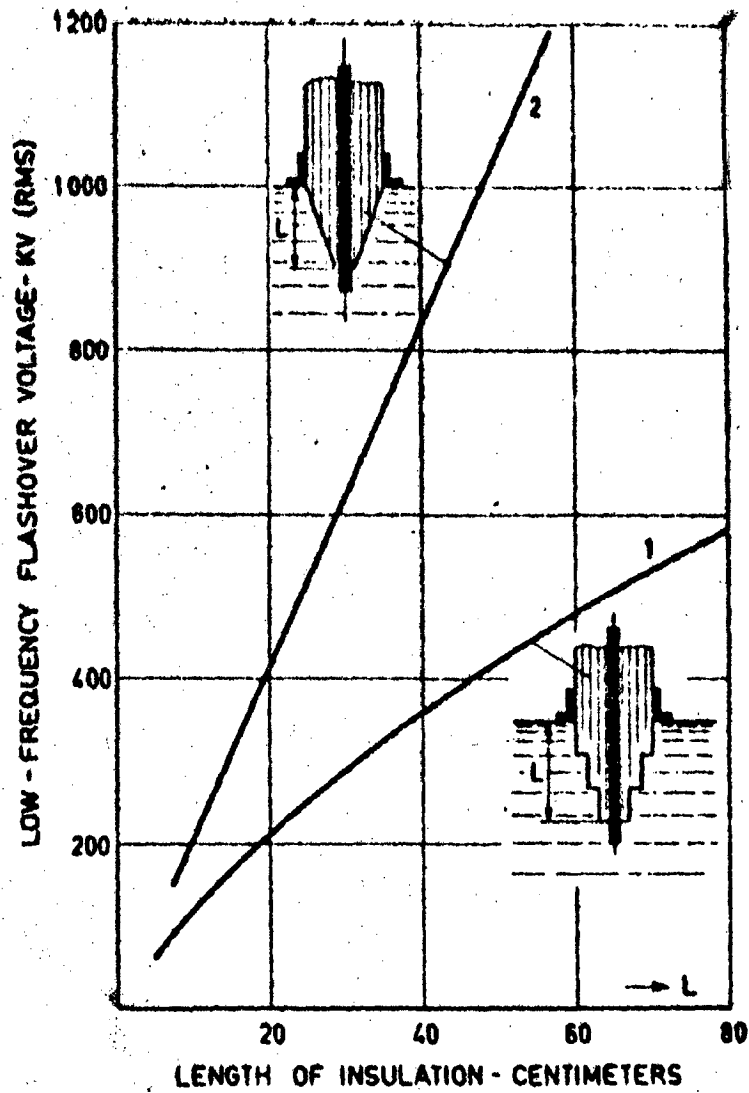
Fig. 4.- Low-frequency flashover under oil of resin-bonded paper bushings. Curve 1—bushing with embedded condenser layers. Curve 2—bushing with free edges of condenser layers.
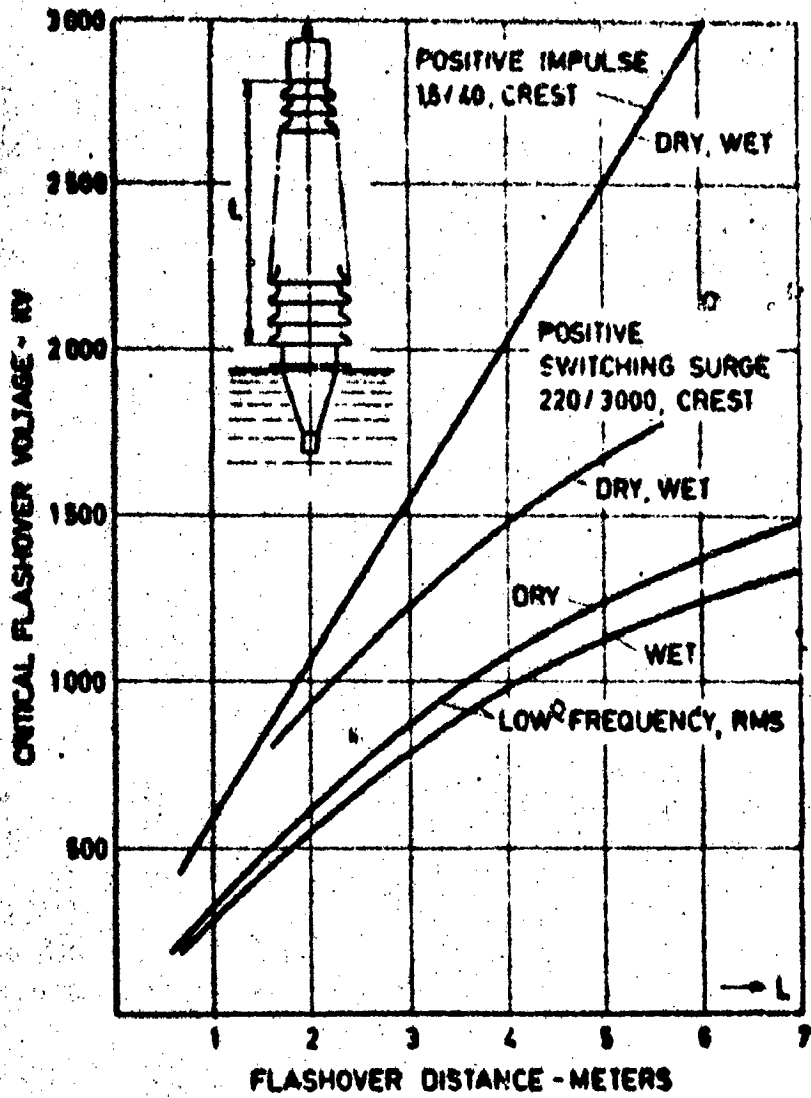
Fig. 5 :- Flashover of bushings in air at standard atmospheric conditions.

frequency voltage diminishes appreciably. The same saturation phenomenon is observed with switching surges whose positive flashover voltages are even some what lower than the peak values of the power frequency flashover voltage.

All these phenomenon indicate that there is a limit to the increase in the system voltage, determined by the considerable growth in flashover distance and the wide dispersion of the measured values. Flashover distances with an rms value of 1600 KV are almost impossible to attain with a reasonably tolerable length. System voltages well above the 1000 KV limit can only be achieved by a substantial reduction of the power frequency and switching surge test levels. Then it is air which imposes the upper limit on system voltages.

1.5   MANUFACTURE OF LARGE INSULATING BODIES:

Bushings for higher voltages are assembled from a number of sections, for thermal and production reasons. This reduces the risk that has to be borne by the manufacturer, as each section can be tested to its full voltage before assembly. When the sections are put together oil gaps are left which are dielectrically short circuited, so that the oil is not subjected to any electrical stresses.

In this way the manufacture of bushing for EHV
range is quite complicated.

1.6 ATMOSPHERIC POLLUTION EFFECTS AND MOISTURE INFLUENCE:

One of the main causes of high failure rates or damage
in number of designs of bushing is an increase in the
moisture content of the internal insulation, which bui-
lds up during operation, to comprise 4-5 % of the
weights of the paper or which is due to a technical
failure (up to 1-1.5 percent by weight). Complete
reliability of bushings in relation to flashover must
be achieved by hermetically sealing the part, improving the
manufacturing techniques, avoiding contamination by
insulating material and avoiding moisture absorption.

Salt deposits in coastal regions is also a signifi-
cant problem in case of bushings. But, if a conductor
barrier is inserted into the flashover discharge path
which is wetted by salt dissolved water, the flashover
voltage can be raised.

2.0 SOME EXISTING BUSHING TYPES:

1. 110 KV condenser wall bushings

2. Elephant type EHV Bushings

3. Air to SF_6 and Oil to SF_6 Bushing Using a
   special resin inpregnated paper, system. [RIP system]

2.1 110 KV CONDENSER WALL BUSHINGS (SIEMENS) [2]

The continously growing demand for electrical
energy has led to load concentrations particularly in
large cities and industrial centres. A transition is
also taking place towards distribution networks of higher
voltages. The primary distribution level that is gene-
rally choosen is 110 KV. The lack of suitable sites,
together with the high price of land, town planning
aspects and the pollution conditions have resulted in a
steady increase in the number of indoor installations.

In order to bring bare high voltage conductors
through the walls and ceilings of indoor stations,
condenser wall bushings are required. Since the indoor
station are mainly built for an insulation rating of
110KV a new indoor bushing and a wall bushing leading from
outside to inside the station with an insulation rating
of 110 KV have been developed.

The bushing core consist mainly of rolled SRBP or rolled soft paper impregnated with oil or epoxy resin. For outdoor applications, the bushings are provided with ceramic jackets. The hollow space between the bushings core and the ceramic jackets is generally filled with oil or bitumin. Expansion vessels are generally required to take up the thermal expansion of such fillings. Furthermore a definite inclination is prescribed for transport and mounting.

The bushings are of indoor-indoor type and outdoor-indoor type and have an impulse withstand voltage of 450 KV and having a rated current of 1250 A.

There is little point in using two different insulation ratings for a piece of equipment consisting of an outdoor end and an indoor end since the voltage stresses on both ends are the same. For this reason the outdoor indoor bushing is also designed for this insulatinn rating. This resulted in a very compact design (Fig.6). The power frequency withstand voltages for the outdoor end apply for wet conditions and those for the indoor end for dry conditions.

Construction : The SRBP core with the metal foil potential grading layers is rolled directly over a copper through bolt of 36 mm dia which is terminated at both
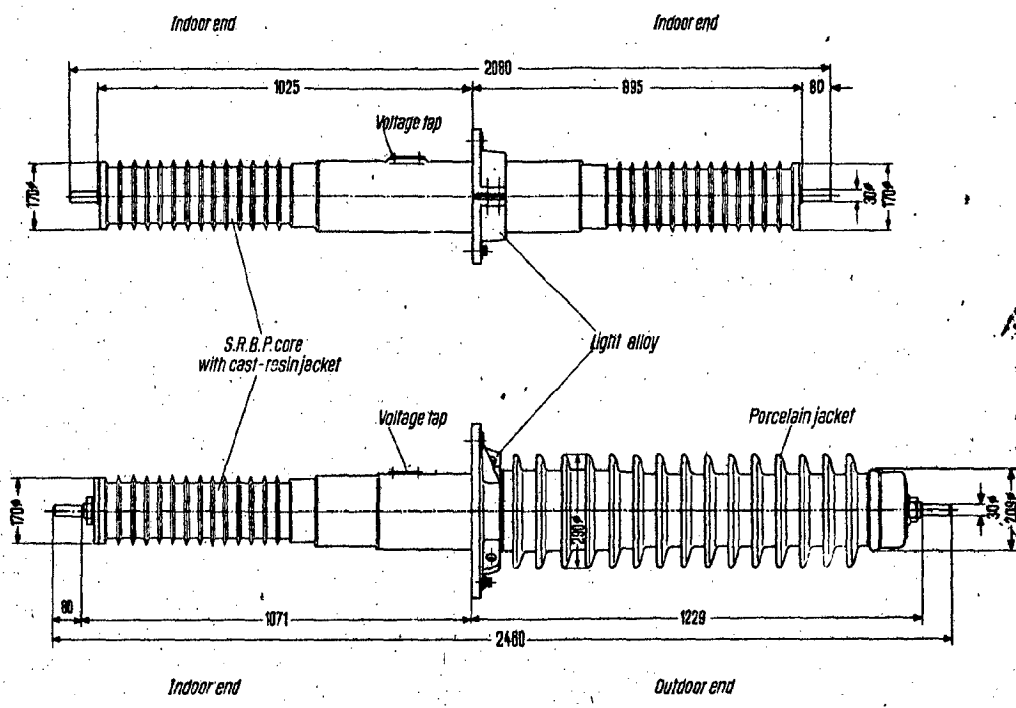
Fig. 6 Dimensions (in mm) of the indoor-indoor bushing DII 110/450-1250 (top) and outdoor-indoor bushing DFI 110/450-1250 (bottom)

ends in a 30 mm dia, 80 mm long connecting stud and

is designed for a rated current of 1250A. In order to

protect the bushing against external influences the

indoor-indoor bushing and the indoor end of the outdoor-

indoor type are provided with a cast resin jacket and

the outdoor end with a porcelain jacket. All jackets are

of cylindrical shape since the surface deposit performance

of this design is much better than that of conical types

as has been proved by post insulators with cylindrical

bodies. For the same reason the porcelain jacket is

provided with a large number of sheds and cast resin

jacket with many ribs. The jacket ensures satisfactory

protection in damp indoor installations, thus also

making the bushings suitable for use in tropical climates

where the atmospheric humidity is very high at many times.

The hollow space between the bushing core and jacket

is filled with SIBIT, a new rubber like compound. This

compound is resistant to low temperatures, is non-

inflammable and does not liquiefy when exposed to thermal

stresses. Its expansion coefficient is so low that the

conventional expansion vessel is no longer required.

The bushing can be transported and mounted in any desired

position. It can thus also be shipped in simple inexpensive

cases. Owing to the sheds of porcelain, jackets with

hanging sheds must be used for bushings which are to
be mounted ·at an angle of 105° to the vertical.

The terminal tapes of outdoor-indoor bushing are
fitted with springs which in conjunction with rubber
gaskets, hermetically seal the bushing core. The bushings
are therefore not cemented. The support flange is of
light alloy. It is split in the case of completely indoor
bushing and is clamped directly over the cast resin
jacket. Connected to the light alloy flange is an earthing
layer so that in the case of indoor -indoor bushing the
earthing plate or earthing frame can be dispensed with.

For measuring purposes, all bushings are provided
with a capacitance tap outlet between the last metal foil
layer and the earthing layer, but this is normally short
circuited.

TABLE NO 1

DETAILS OF 110 KV BUSHING

Characterstics	DII 110/450-1250	DFI 110/450-1250
Insulation level	110 KV	110 KV
Highest System Voltage	125 KV	125 KV
Impulse Voltage withstand 1/50 full wave	450 KV	450 KV
Power freq. voltage withstand 50 c/s (indoor end dry, outdoor end wet)	230 KV	230 KV
Rated current	1250 A	1250 A
Rated short time current (1 sec).	50 KA (rms)	50 KA (rms)
Centilever strength	375 Kg.	375 Kg.

DESIGN DATA

Weight	50 Kg..	142 Kg.
Indoor End		
Arching distance	800 mm	800 mm
Total Creepage distance specific Creepage distance (referred to 110 KV)	1170 mm 1.07 cm/KV	1170 mm 1.07 cm/KV
Number of ribs	15	15
Pitch of ribs	32 mm	32 mm
Projection of ribs	15 mm	15 mm

Design Data	DII 110/450-1250	DFI . 110/450-1250
Outdoor End		
Arcing distance ·	-	1000 mm
Total Creepage distance	-	2266 mm
Specific Creepage distance (referred to 110 KV)	-	2.06 cm/KV
Protected Creepage path in rain at 45 deg.	-	1360 mm
Number of sheds	-	15
Pitch of sheds	-	65 mm
Projection of sheds	-	55 mm

2.2 EHV ELEPHANT TYPE BUSHING : [1]

Recent cooperative development by representatives of electric machine and cable manufacturers in Japan has resulted in direct connected combination of high voltage cable, Pot head and transformer, designated as EHV elephant type bushing. With all connections from transformer to cable under oil, dimensions and space requirements are reduced, and problems of atmospheric contamination and flashover are eliminated.

Oil filled cable is not commonly used because of its expense contrasted to overhead lines. However, there are cases where its use can be justified such as with the new elephant type bushings on some installations in Japan, where further applications are contemplated;

(i)   In growing cities, the use of power has been increasing so that ever high voltages are warranted.

(ii) Hydro electric power is often located at dams in steep mountainous terrain, where underground power station have been found more favourable and the power is brought by cable from transformer to the surface. Again the combination of cable and elephant type bushings reduces the space requirement.

(iii) Recent large steam power stations have been constructed adjacent to seashores for reasons of land availability and convenience in fuel transportation. For such application, salt contamination is heavy and practical countermeasures are difficult. Cable and elephant type bushings avoid the contamination problem when the cable transmission ends inland or at some indoor substation.

Construction and Features: [Fig.7]

There are two general methods of connecting the pothead into the transformer tank (i) by direct connections

DIRECT TYPE

CONNECTION BOX

POTHEAD

OIL

CABLE

WALL BUSHING

CORE B
WINDING

TANK
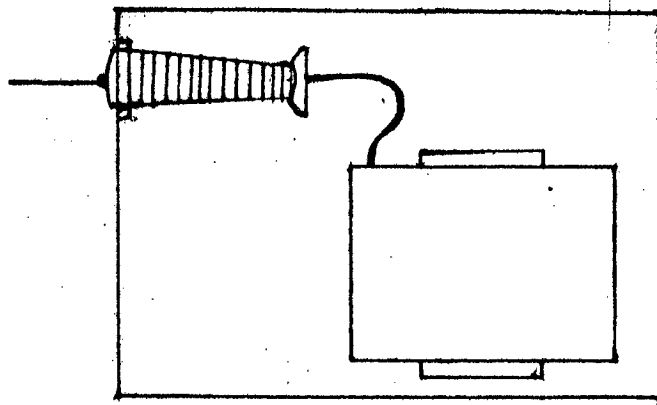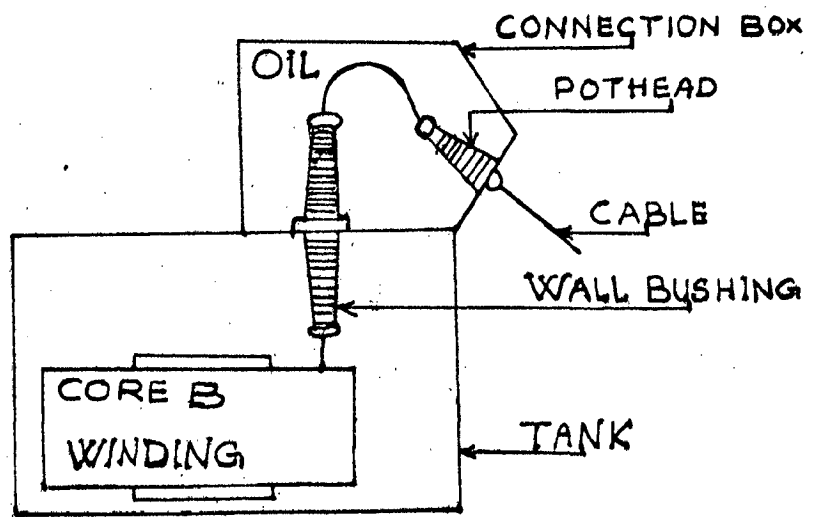
INDIRECT TYPE

Fig.7:-ELEPHANT-TYPE ARRANGEMENTS

of potheads to the transformer winding and (ii) by housing a separate oil compartment connecting through a wall bushing into the transformer. These are designated respectively as direct and indirect types. The direct type obviously reduces dimension and is less expensive, but has some disadvantages: (1) Trouble in the cable or transformer may involve both. (2) The transformer oil must be drained for inspection and repair of the potheads and (3) Cable and transformer winding cannot be separately tested after installations as for example, d.c. tests on the cable.

The combination of high voltage oil immersed potheads mounted on the transformer designated as elephant type bushings, offer three main advantages over conventional type bushings.

(i) <u>Economy of Space</u> :

Since the transformer-to-cable connection is made under oil, the dimension and space requirements can be greatly reduced. With the application of shields, insulation clearances may be as low as one tenth of those required for air-type bushings and potheads. Therefore even with indirect type construction, the space of the transformer vault will be substantially smaller.

(2) Weather Proofing :-

The elephant type bushing having no exposed live parts, is entirely free from atmospheric contamination and is therefore highly advantageous for power stations located on the seashore, particularly for those in the range of EHV transmission voltages.

(3) Service Reliability :

Absence of exposed live parts make indoor installations safe from electrical hazards. In the case of indirect type, housing separate oil filled compartments for each pothead, any trouble due to equipments failures can be better restricted to its local origin. A relief vent on each pothead compartment, prevents trouble in other phases or equipment.

2.3 AIR TO SF_6 AND OIL TO SF_6 BUSHINGS USING A SPECIAL RIP SYSTEM : [6]

Like some other bushing manufacturers Felton and Guillaume Dielectra have established a programme of air to SF_6 and oil to SF_6 bushings using a special RIP system under the trade mame Pertinex -100 (P X 100).

Characterstics of P X 100 : The P X 100 main insulating body consists of a structure of high grade insulating paper impregnated with epoxy resin. The condenser layers of aluminium foil are inserted into the winding body during

Air to SF$_6$ Bushings :

P x 100 bushings are being used in SF$_6$ switch. - gears. Fig. 8, shows 123 KV air entrance bushings on a German substation in a heavy polluted area. Due to the condenser field grading, a very slim line design is possible. The porcelain envelope preferably is of cyclindrical shape with a narrow gap between its internal surface, leads to a minimum gas volume inside the porcdlain and consequently to reduced devastation in case of porcelain damage. Via channels through thd flange, the bushing gas communicates with the gas of the bus duct.

Fig. (8) drawn earlier shows that the conductor is fixed at the lower end of main insulating body and is connected by sliding contacts to the top armature of the bushing. This offers the advantage to apply static seals without relative movements due to different thermal dilations. The design is applicable for rated currents upto 2500 A at 245 KV and 2000 A at 420 KV.

Because the electrical main insulation of a condenser bushing is at the same time a thermal insulation and thus limits the current carrying capacity of conventional conductors. The range of higher currents is covered by special conductors which carry the heat generated by the electrical losses in the axial direction

the winding process. The geometry and positioning
of these layers are obtained by a computer in such a way
as to ensure minimal electric stress along the surface of
insulating body immersed in gas.

After the winding process, the wound body is dehydrated
and impregnated with epoxy resin under vacuum. In order to
achieve a total impregnation and to avoid internal
mechanical stresses due to the shrinkage of the resin during
the curing and cooling procedure, a special crepe paper
is used. Thus the main insulation is free of voids and
inherently gas tight.

The choice of the number and radial distance of
condenser layers determines the electric strength within
the insulating material. This choice is to be taken by
considering the withstand strength of the relevant
material. For P X 100 endurance tests were carried
out on samples and on full size bushings. For the purpose
of accelerating the ageing process, the applied field
strength was chosen within the range of 7.5 KV/mm and
13 KV/mm, these values being far above the operational
stress. Thereby the end of the life time of the test
objects was defined by the puncture through the insula-
tion between two adjacent condenser foils, this being
detected as a sudden change in capacitance by a self
balancing schering bridge.

1. Connection & top armature.

2. Flang with adhesion in epoxy resin.

3. Sliding contact.

4. Current Conductor.

5. Main insulating bod of PX100.

6. Monopiece porcelin envelope.

7. Oring seat.

8. Gas channels.

9. Measuring tap.

10. Adaptar housing.
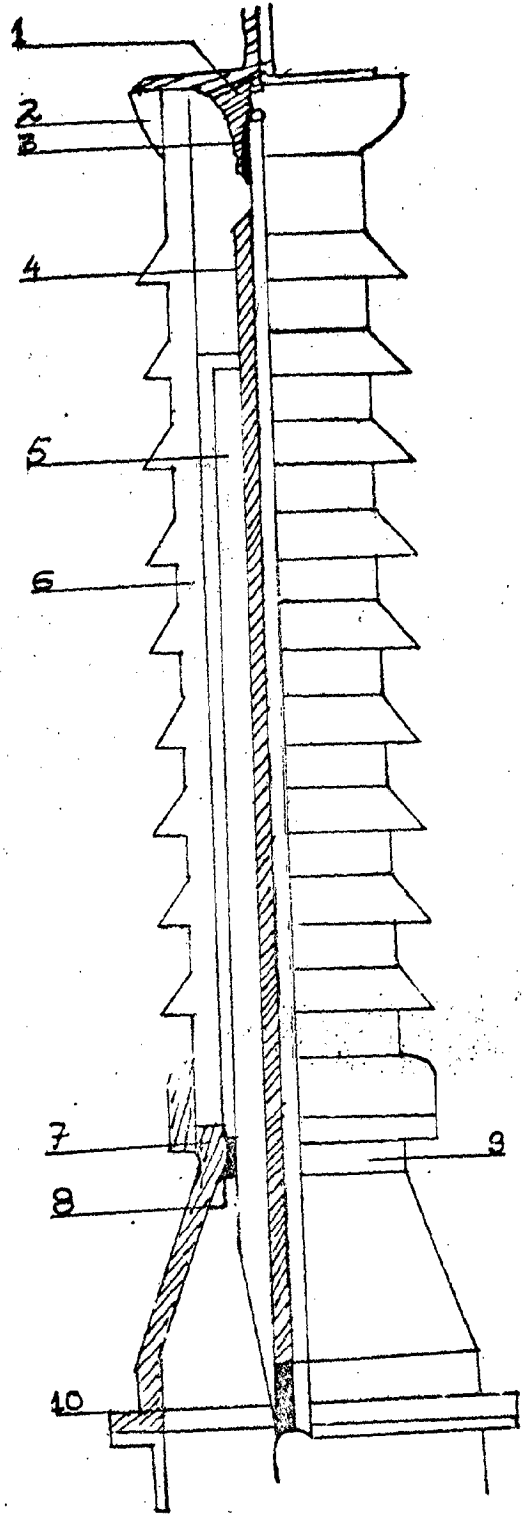
Fig:8:- Sectional View of a SF6 Outdoor Bushing.

to the outdoor end of the busing. There the heat is
dissipated by a radiator which is firmly attached to the
current conductor. The internal heat transmission takes
place following the heat pipe principle. This operates
by the evaporation of a heat transfer agent in the hot
area of the conductor and the condensation of the same
agent in the radiator area. The great advantage of this
process is that heat is transferred with a minimum tem-
perature gradient.

Bushings of a compact design for a rated voltage
of 420 KV and a rated current of 4000 A are economically
built by means of this cooling technique.

For indoor application e.g. when testing sub-assemblies
in the factory or on site, it is advantageous to use
P X 100 bushings without porcelain envelope; hereby the
weight is considerably reduced.

Because of the necessary length of the grounded
flange part, the roof bushing is composed of a normal air
entrance bushing, an SF_6 duct and an indoor bushing without
precelain.

Oil to SF_6 Bushings:

P x 100 offers particular advantages when used for oil
to SF_6 bushings intended for the direct connection between
power transformers and metal enclosed switchgears. This
is due to the absence of any impregnating liquid in the

main insulating body and consequently the absence of space consuming porcelain envelopes, together with necessary compensation devices.

The question of gas tightness of air to SF_6 bushing is mainly an economical question. All seals must keep the leakage rate on a low level in order to save SF_6 gas.

For the oil to SF_6 bushing the problem of gas tightness is technically relevant. Although it is not finally clarified, it is a common opinion that the decreasing solubility of SF_6 in oil with increasing temperature and possibly generated decomposition products of SF_6 due to arcs in the tap changer cause additional insulating problems within a transformer with SF_6 contaminated oil. Therefore the gas tightness is one of the most important requirements for oil to SF_6 bushings.

Resin impregnated paper is inherently imprevious and does not permit any penetration of gases or liquids. Consequently only the interfaces between the main insulating body and the conductor and the main insulating body and the flange have to be sealed.

At the flange this is effectuated by static seals in a similar way as with air to SF_6 bushing and the eventually leaking gas can escape into the surrounding air via an annular chamber in the flange.

A penetration into the transformer is not possible because the gas in the annular chamber is not under pressure.

At the conductor the eventually leaking gas cannot be bypassed into the air and therefore the sealing system must be redundant or absolutely fatigueless. This can properly be achieved by the application of a trap which is filled with a silicone oil of extreme high viscosity. This kind of sealing system is well approved in the vacuum technology for the sealing of moving parts.

3.0 THERMAL PERFORMANCE OF BUSHINGS :

Although the practice of loading transformers beyond nameplate rating has been gaining wide acceptance over the past 30 years, very little attention has been given to the overload capability of bushings. In spite of the fact that there have been few, if any reports of bushing service difficulty as a result of transformer overloads, there is a growing feeling of insecurity with regard to bushing over-load capabilities. This concern is brought about by the universal acceptance of 65° average winding rise transformers and an increasing dissatisfaction with the concept that the ancillary equipment may limit the overloads permitted by the Power Transformer Loading Guides.

Three possible failure modes can be identified as potential problems in a less conservative design or application practice. All three of these could result in dielectric breakdown of the bushing.

(i) Thermal degradation of insulation resulting in an accelarating increase in dissipation factor.

(ii) Oil expansion causing internal pressure to build up to a level sufficient to blow out a gasket.

(iii) Gasket hardening from high temperature resulting an ultimate loss of seal.

Although failure by any of these three modes would not necessarily occur at the time of an excessive overload,

the detoriation effects would be cumulative. Unless preventive maintenance detected the changing condition of the bushing the consequence could range from an unplanned outage for bushing replacement to serious damage to the transformer. In view of the above, there is a need to develop the thermal model of the bushing to calculate overload performance.

3.1 DEVELOPMENT OF MODEL ARCHITECTURE : - [5]

In order to adequately predict bushing performance under variations in boundary temperatures and system load, at least three operating parameters should be known. First, a fairly accurate assesment of the hot spot temperature of the bushing conductor must be made in order to determine possible damage to insulation. Second, a means of estimating the average oil temperature in the bushing oil duct is necessary to determine the possible pressure buildup in the closed vessel. Third, the variation of the temperature profile with respect to time must be approximated in order to determine the effects of short time load peaks. A compromise has been made in the method of calculating transient behaviour to reduce potentially excessive development costs. Rather than attempt to calculate transient performance directly, a thermal model is used to calculate the steady state temperature. The transient temperature can then be predicted by utilizing data on time constant obtained from rated current heat runs. This scheme somewhat reduces model complexity.

To meet the criteria outlined above, the finite difference model was developed [Fig.9.]. The bushing has been divided axially into eight nodes. The number is a compromise between model accuracy and computing costs . For units above 196 KV voltage class the number of axial nodes would probably have to be increased. Radially the bushing has been sectioned to provide three sets of nodes, one to provide a thermal profile of the conductor, one to interface the bushing with its operating environment and one to provide an estimate of average temperature in the oil dact. The results of this sectioning reduce the bushing to a group of hallow cylinders which can be described in cyclinndrical coordinates (r, Θ, z). The bushing temperature distribusion is assumed to be independent of Θ , and the solution therefore becomes two dimensional. The familiar analogy between fourier's law for heat flow and ohm's law for the flow of electrical current can be stated as

$$Q = \frac{\Delta T}{R_t} \quad \text{is analogous to} \quad I = \frac{\Delta V}{R_e}$$

where,

Q = Heat transfer (watts)

ΔT = Temperature change Across R_t($^{\circ}$C).

R_t = Thermal resistance ($^{\circ}$C/watt)

I = Electrical current (Amps)

ΔV = voltage change across R_e (volts).

R_e = Electrical resistance ohms).
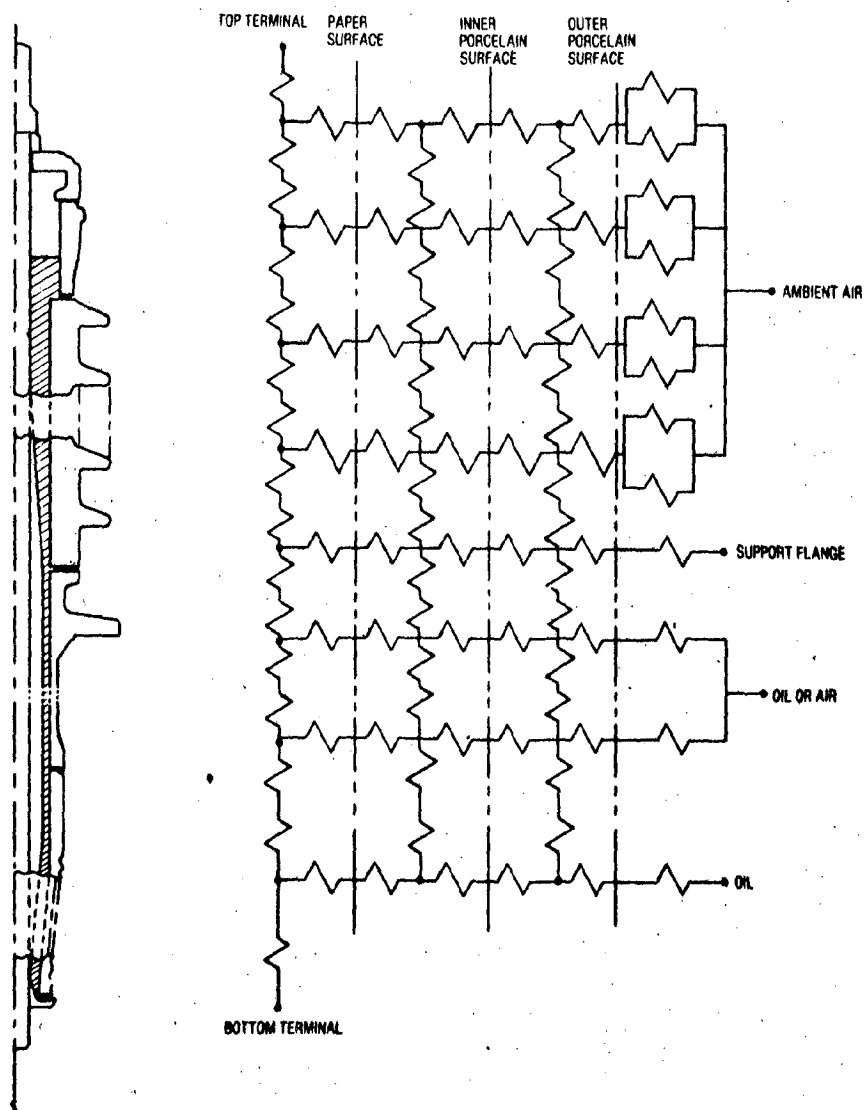
Figure 9 — A Finite Difference Model For Predicting Bushing Thermal Performance.

The thermal ckt is converted to an electrical
network which ca$_n$ then be solved by applying Kirchoff's
current law for electrical ckts.

Σ Q node $= 0$ or ΣI node $= 0$

The resulting finite difference equations for the
network in matrix notation, are of the form

$$[K]\ [T] = [Q]$$

K = network element conductance matrix

T = nodal temperature matrix

Q = internal heat generation and boundary heat
transfer matrix.

A computer algorithm which employs Gaussian
elimination, is used to solve the matrices to get

$$[T] = [K]^{-1}\ [Q]$$

Boundary conditions representing the interface between
the bushing and its environment must also be considered.
The present model requires all boundary temperatures
to be specified. These are the air end terminal, oil end
terminal, support flange, immersion oil and ambient air.
These temperatures are divided by their corresponding boundary
resistances to determine the resultant heat transfer at the
boundaries. Heat transfer quantities are then entered into
the [Q] matrix to be used in obtaining a network solution.

In order to correlate temperature profile predictions
with available test data, boundary temperatures measured
during corresponding heat runs were used in model cal-
culations. In the general case however, the top and bottom
terminals and support ɿflange temperatures would not be
known for the loads other than design rating. Immersion oil
temperature can be obtained from equipment manufacturers
for various loading conditions, but presently estimates of
the other boundary temperatures have to be made based upon
what-ever heat run data is available. Further plans for
the model include the modeling of air bus work, the
transformer cable and the transformer cover, so that the
bushing terminals and support temperatures can be calculated
directly.

3.2 ESTABLISHMENT OF MODEL PARAMETERS : [5]

Following developments of modeling scheme it becomes
imperative of accurately determine the values of network
elements. In the case of thermal conduction resistances
the approach is straight forward. The formulae employed
for the calculation of radial and axial conduction in
coaxial cyclinders being,

Radial Axial

$$R_t = 1/[2\pi \ell K / \ell n (r_o/r_i)],\qquad R_t = \ell/\pi K (r_o^2 - r_i^2)$$

where,

R_t = thermal resistance ($^\circ C$/watt)

K = thermal conductivity ($watts/in^2/^\circ C/in$)

ℓ = nodal length in axial direction (in)

r_o = outer nodal radius (in)

r_i = inner nodal radius (in)

The values used for the thermal conductivity K are obtained from the handbook tables for the materials under consideration.

The heat transfer at solid fluid interfaces is calculated using correlations derived from MC Adam's for free convections from vertical surfaces. For air, the equation for thermal resistance is,

$$R_t = \frac{1}{0.0085 \; As \; (T_s - T_a)^{1/3}}$$

where,

T_s = Surface temperature ($^\circ C$)

T_a = Ambient temperature ($^\circ C$)

As = Surface area of the node (in^2).

This relationship is applicable for the turbulent flow which is applicable for the range of bushings under consideration.

For solid -oil surfaces, the equation used is of
form

$$Nu = A \ (G_r \ P_r)^B$$

where,

$Nu = h\ell/K = $ Nusselt number

$$Gr = \frac{p^2 \beta \ g \ \ell^3 \theta}{\mu^2} = \text{Grash-of number}$$

$Pr = C_p \ \mu/K \qquad = $ Prandtl number

$\rho \ = $ oil density

$\beta \ = $ thermal expansion coeff.

$g \ = $ gravitational constant

$\ell \ = $ length of node

$\theta' = $ surface to fluid temperature difference

$\mu \ = $ dynamic viscosity

$C_p = $ specific heat

$\bar{h} = $ average heat transfer over the surface

For $G_r \ P_r \leq 10^4$, $\quad A = 1.5$ and $B = 0.14$

(derived from Mc Adam's curve)

For $G_r \ P_r > 10^4 \leq 10^9$, $\quad A = 0.59$ and $B = 1/4$

For $G_r \ P_r > 10^9$, $\qquad A = 0.13$ and $B = 1/3$

The expression for the thermal resistance for surface
to oil convection then becomes.

$$R = \frac{\ell}{K \ A_s \ Nu}$$

This relationship is assumed to apply whether heat
is being transferred from surface to oil or from oil to
surface (either heating the oil or cooling the oil).

Radiation from the busing surface 'to 'its surroundings
is also treated as a thermal resistance. The relationship
used is

$$R = \frac{T_s - T_a}{\sigma \, \varepsilon \, As \, [\, (T_s + 273)^4 - (T_a + 273)^4]}$$

where

σ = Stefan - Boltzmann constant

$(= 3.66 \times 10^{-11} \, watts/in^2 \, (^\circ K)^4)$

ε = surface emissvity

The equation assumes the radiation environment is at
ambient air temperature. It does not account for either
solar or nocturnal radiation. It also assumes that the
surroundings are perfect- radiators, and absorbers, and
the surface sees a uniform environment. These assumptions
are approximately correct for indoor test facilities.
Unfortunately, material properties used in establishing
network resistances are temperature dependent. In addition
convection and radiation terms make the thermal differential
equation non linear. By applying an iterative solution
technique, however, it is possible to consider them as
th-ough they were linear. This is accomplished by assuming
an initial temperature distribution which is used to

calculate coefficients (thermal resistances including temperature dependent material properties, convection and radiation) for the set of linear equations. The solution of those equation yields a new temperature distribution which is used to re-evaluate material properties and the **thermal** resistances. The new resistances are used to obtain a new solution for the temperature distribution. The process is repeated until the change between successive temperature solutions is judged sufficiently small.

Calculations for network elements considered thus far are applications of the text-book formulae for the various forms of heat-transfer. Axial convection in the bushing oil duct is an extremely complicated phenomenon in which the direction of the flow appears to vary with the temperature (Fig. 10). Solution via a classical approach (solving the Navier- Stokes equations) would be costly to calculate. This raises a question as to whether a simple emperical technique might provide reasonable results for less cost. One such technique considered was to assume that the axial convection resistance is inversely proportional to the cross-sectional area of the duct.

$$R_t = C/Ac$$

where

$$R_t = \text{Thermal resistance (ohms)}$$

$$C = \text{Constant}$$

$$A_c = \text{Cross sectional area at node (in}^2)$$

OIL

CONDUCTOR

PORCELAIN (AIR)

PAPER

FLANGE

PORCELAIN(OIL)

A

OIL

CONDUCTOR

PORCELAIN(AIR)

PAPER

FLANGE

PORCELAIN(OIL)

B
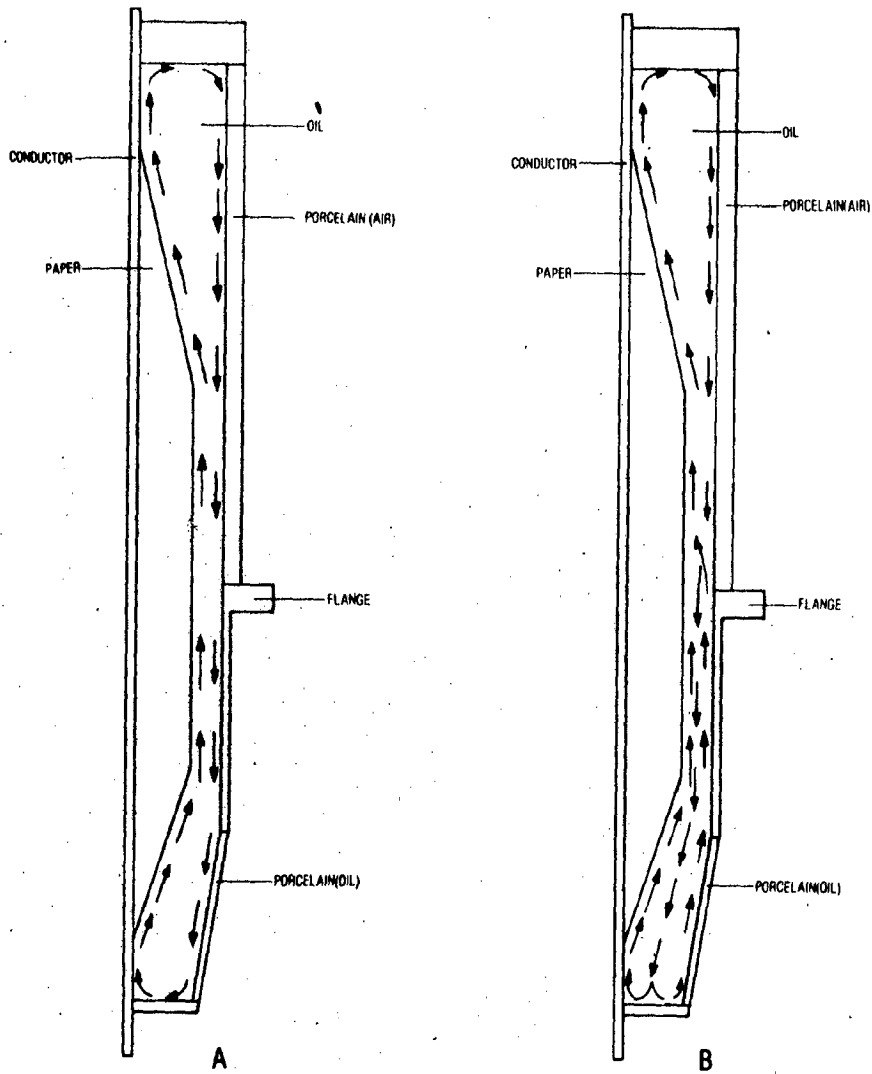
Figure 10 :- Direction of Heat Flow When (A) Transformer Top Oil Temperature <
Bushing Oil Temperature (B) Transformer Top Oil Temperature >
Bushing Oil Temperature.

Applying this technique is merely a matter of determining the correct constant of proportionality. It was realized that this approach would be crude at best. However, it was felt that the hot spot might not be a strong function of the duct oil temperatures because of the large build up for poor thermal conductivity paper on the core rod. In attempting to apply this simplified concept of duct resistance, it was determined that a constant could be found for each bushing that would make predictions track measured data reasonably well. This method is practical if one is interested in predicting overload behaviour and one has rated current heat run data available with which to time the model. In the absence of this data, however one constant was choosen to apply to all units in the scope of the project. Although the predictions for the overall temperature profiles using one constant for all bushings were not as good as using a different constant for each bushing, hot spot temperature predictions changed little. This supported the hypothesis that duct oil temperature has little effect on hot spot temperature. In spite of the fact that the present solution technique appears workable, future improvements should include a refined means of calculating axial duct oil convection, in order to improve the physical relevance of the model and improve its ability to predict average bushing oil duct temperature as well as hot spot.

3.3 A SIMPLE THERMAL STEADY STATE MODEL: [4]

The very sophisticated mathematical model for predictions of bushing thermal performance appears to be too complex to be of practical use in a loading guide. However, it suggests the possibility of a very simple model having only a few elements (Fig.11).

θ_A = Ambient temperature $^\circ C$

θ_T = Steady state top terminal rise over ambient $^\circ C$

θ_B = Steady state bottom terminal rise over oil $^\circ C$

θ_O = Steady state Oil rise over ambient $^\circ C$

θ_{HS} = Steady state Bushing Hot Spot rise over ambient $^\circ C$

Q = Per unit internal heat generation (Internal heat generation at bushing rated current as base)

I = Per unit load current based on bushing rating.

G_A = Equivalent thermal conductance (E.T.C.) Hot Spot to Air.

G_O = E.T.C. - Hot Spot to Oil

G_T = E.T.C. - Hot Spot to Top Terminal.

G_B = E.T.C. - Hot Spot to Bottom Terminal.

In general, internally generated heat would flow from the bushing hot spot outward to the top terminal, to the surrounding air, to the oil in which the bottom end is immersed, and to the bottom terminal (although heat flow between the internal hot spot and the oil or bottom terminal could be reversed for cases of small load current).

**Top
Terminal**

$\theta_T + \theta_A$

$Q = I^2$

G_T

Air
θ_A

G_A

Q

G_O

$\theta_{HS} + \theta_A$

G_B

Oil
$\theta_O + \theta_A$

$\theta_B + \theta_O + \theta_A$
**Bottom
Terminal**
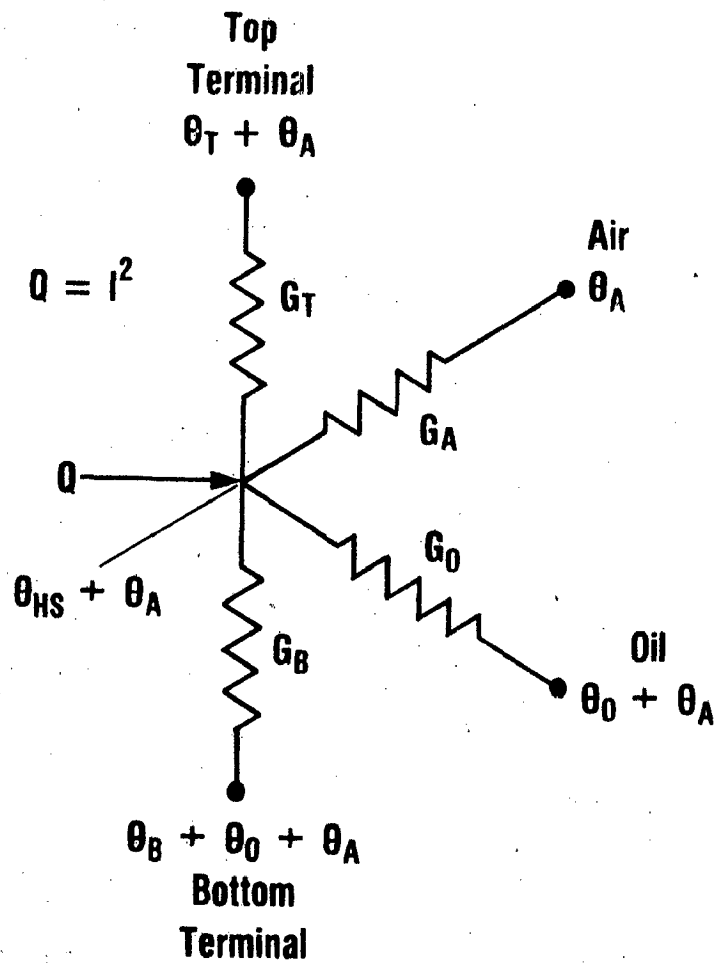
Figure II-A Simple Electrical Analog Model of Heat Transfer in a Bushing.

θ_B = Steady-State Bottom Terminal Rise Over Oil - °C

θ_O = Steady-State Oil Rise Over Ambient - °C

θ_{HS} = Steady-State Bushing Hot Spot Rise Over Ambient - °C

Q = Per Unit Internal Heat Generation (Internal heat generation at bushing rated current as base)

I = Per Unit Load Current Based on Bushing Rating

G_A = Equivalent Thermal Conductance - Hot Spot to Air

G_O = Equivalent Thermal Conductance - Hot Spot to Oil

G_T = Equivalent Thermal Conductance - Hot Spot to Top Termi-minal

G_B = Equivalent Thermal Conductance - Hot Spot to Bottom Terminal

A heat balance equation can be written equating the internally generated heat to the sum of the heat flow through the several branches.

$$Q = G_T (\theta_{HS} - \theta_T) + G_A (\theta_{HS})$$
$$+ G_0(\theta_{HS} - \theta_0) + G_B (\theta_{HS} - \theta_B - \theta_0) \qquad ...(A)$$

Putting $Q = I^2$, and solving for θ_{HS}

$$\theta_{HS} = \frac{I^2 + (G_0 + G_B) \theta_0 + G_T \theta_T + G_B \theta_B}{G_T + G_A + G_0 + G_B} \qquad ...(B)$$

In turn, this equation can be rewritten as

$$\theta_{HS} = K_1 I^2 + K_2 \theta_0 + K_3 \theta_T + K_4 \theta_B \qquad ...(C)$$

This is a very practical form for loading guide use, since it requires only the definition of four K constants, which can readily be defined based on the results of heat run tests for at least four values of load current. The heat run data would be substituted into Eq. (A) yielding four equations involving four G constants. The simultaneous solution of these four equations would define the G constants and would permit determination of K constants. If more than four sets of heat run data are available, a linear regression analysis can be performed to establish the best fitting set of K constants.

A set of heat run data for a General Electric Company 7B590 bushing (69 KV-1200 Amps) has been listed in Table 2.

Data from tests number AO, A1, B4 and E2 are used to define γG and K constants. The results are .

$$G_0 = -.01843 \qquad\qquad K_1 = 30.85$$

$$G_T = -.02773 \qquad\qquad K_2 = 0.857$$

$$G_B = .04620 \qquad\qquad K_3 = 0.856$$

$$G_A = .03237 \qquad\qquad K_4 = 1.425$$

Substituting these constants into equation (C) gives

$$\theta_{HS} = 30.85 \ I^2 + 0.857 \ \theta_0 - 0.856 \ \theta_T + 1.425 \ \theta_B$$

$$\dots(D)$$

When equation (D) is applied to all rows of data in table 2, The calculated values of θ_{HS} is the Calc (a) Calumn results. Comparison with the tested values of θ_{HS} in the immediately preceeding calumn show moderately good agreement.

When all the data of Table is entered in a linear regression analysis equation (E) results

$$\theta_{HS} = 30.40 \ I^2 + 0.718 \ \theta_0 - 0.204\theta_T + 0.152 \ \theta_B - 1.4$$

$$(E)$$

The calculated results for all test conditions are listed in Calc(b) calumn. The values are now more closer to experimental values. Thus, it is shown that the simple bushing model have adequate accuracy as we are getting the values very near to the experimental values.

Table 2

Thermal data from heat runs performed by southern California Edison Company on a General Electric Company 7B 590 bushing (69 KV, 1200 Amps)

Test No.	I^2(p.u)	θ_0	θ_T	θ_B	θ_A	θ_{HS}	Calc θ_{HS}(a)	CalC θ_{HS}(b)
-	0	0	0	0	-	0	0	-1.4
A0	0	38	10	0	32	24	24.0	23.8
A1	1.00	40	28	9	30	54	54.0	53.3
A2	1.44	36	33	11	33	61	62.8	63.1
A3	2.56	36	51	20	33	93	94.7	94.9
B0	0	56	15	0	31	36	35.2	35.7
B1	1.00	55	29	9	31	63	66.0	63.9
B2	2.56	51	54	23.0	34.	106	109.3	105.5
B3	4.00	52	71	30	34	150	150.0	147.6
C0	0	58	16	0	30	37	36.0	37.0
C1	1.00	57	36	10	30	65	63.2	64.1
C2	2.56	53	60	22	33	107	104.4	105.6
D0	0	59	16	0	29	36	36.9	37.7
D1	1.00	57	31	10	31	63	67.5	65.1
D2	2.56	54	56	21	33	105	107.3	106.9
E0	0	67	20	0	27	44	40.3	42.6
E1	1.00	66	35	9	27	73	70.3	70.6
E2	2.56	62	58	20	32	111	111.0	112.1

4.0 DESIGN PROCEDURE FOR 750 KV, 2000A OUTDOOR - IMMERSED BUSHING :

In the simplest form a bushing would be a cyelinder of insulating materials with radial clearances large enough to suit the electric strengths of the insulating material and axial clearances depending upon the electrical strengths of surrounding media. In these types a bushing voltage is not evenly distributed through the wall thickness of the insulating material or along the axial length of the insulation (Fig. 12). Since the dimensions of the bushings would become very large as the voltage increases, these bushings cannot be used at high and extra high voltage levels.

To overcome this difficulty the condenser bushings are used where the wall thickness is divided into a number of capacitors by concentric conducting cyelinders. In view of insertion of concentric capacitors uniform voltage distribution is achieved. The uniformity in voltage distribution facilitates the reduction in the dimensions of the bushing thus resulting in economy of floor space, size of the tank, quantity of oil used etc. (Fig 13)

Condenser bushings are broadly divided into two types namely synthetic Resin Bonded Paper type and Oil Impregnated Paper type. In OIP bushings the partial discharge level is comparatively lower than SRBP bushings and also full width of resin coated paper is not available for extra high voltages.
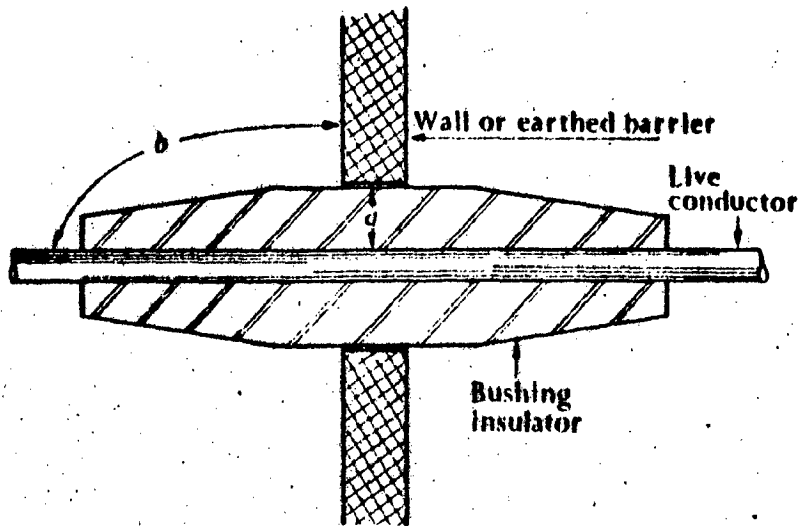
Fig. 12 (A) Simple bushing.
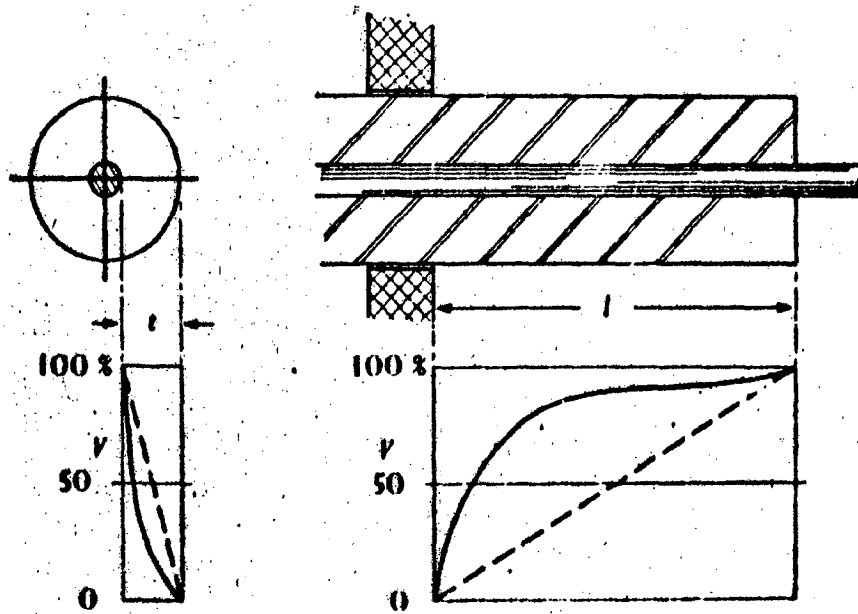
Fig. 12 (B) Voltage distribution in simple bushing.
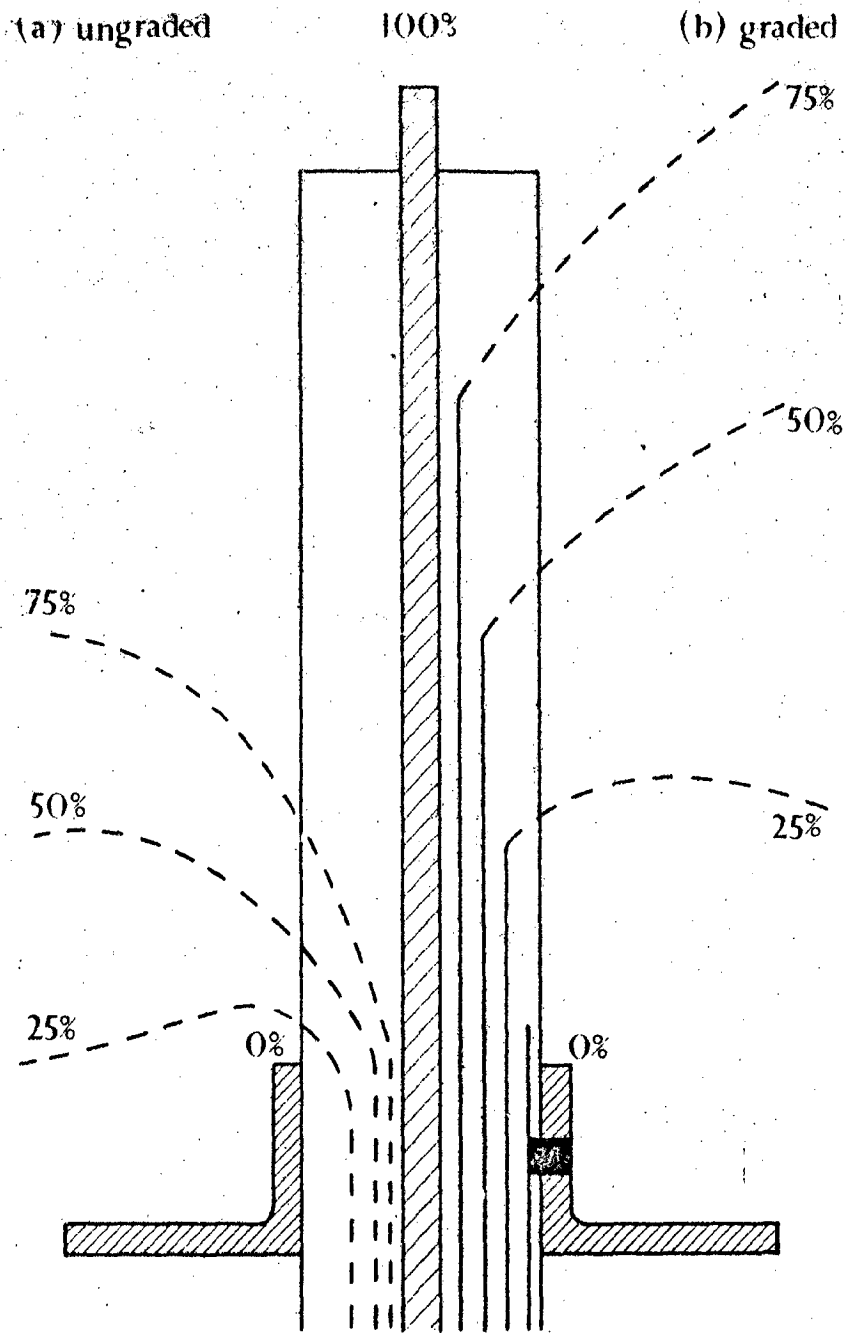
FIG. 13 :— Voltage distribution with and without capacitance grading.

For OIP bushings, even though the full width paper may not be available, the paper tapes can be used. So OIP bushings are the best choice for extra high voltage range.

4.1 THEORY OF CONDENSER BUSHING :

In condenser bushings, around the central conductor, there are a number of layers of impregnated paper insulation, in between them the metal foils are inserted to form a number of condensers in series. If they are designed in such a manner that all the condensers have equal capacitance the potential difference across every capacitor is the same and equal to the total voltage divided by number of capacitors. The capacitance is given by

$$C = \frac{2\pi\epsilon \ L_{r1}}{\ln(\frac{r_1}{r})} = \frac{2\pi \ \epsilon L_{r2}}{\ln(\frac{r_2}{r_1})} = \quad \cdots$$

where

L_{r1}, L_{r2}, ... are the lengths of the successive metal foils starting from the central conductor.

r = radius of the central conductor r_1, r_2,... are the radii first, second,....metal foils.

For capacitance of each layer to be equal

$$\frac{L_{r1}}{\ln(\frac{r_1}{r})} = \frac{L_{r2}}{\ln(\frac{r_2}{r_1})} = \cdots \qquad (1)$$

Grading of radial Stress

The maximum stress in the first condenser which occurs at the conductor surface is

$$E_{1max} = \frac{v_1}{r \ln \frac{r_1}{r}} \qquad (a)$$

where v_1 is the voltage across the first condenser.

Similarly the maximum stress in the second condenser is

$$E_{2max} = \frac{v_2}{r_1 \ln \frac{r_2}{r_1}} \qquad (b)$$

where v_2 is the voltage across the second condenser.

As the capacitance of each layer is the same the potential difference across each layer will be the same, so that

$$v_1 = v_2 = \cdots$$

Now equating the maximum stresses

$$r \ln \frac{r_1}{r} = r_1 \ln \frac{r_2}{r_1} = \cdots \qquad (2)$$

From (1) and (2)

$$r \ln r_1 = r_1 \ln r_2 = r_2 \ln r_3 = \cdots$$

This is the criterion for grading of radial stresses. Subsequently a check is made to ensure that the axial stress between foils along the surface of insulation is not excessive.

Grading of Axial Stresses :

If the above expression is written in the form

$$Lr_N = Lr_1 \frac{r}{r_{N-1}}$$

It is evident that the edges of the equipotentials follow an inverse profile. Since the voltage of the equipotential vary linearly from conductor to flange, the resulting axial distribution is also of inverse form and not uniform. The dimensioning has to be redone if it is desired to have uniform axial distribution.

4.2 CENTRAL CONDUCTOR SIZE :

For a current density for copper of 1.5 A/mm^2, the cross sectional area of the central conductor

$$= \frac{2000}{1.5} \text{ mm}^2$$

$$= 1333.33 \text{ mm}^2$$

This gives a conductor radius r= 20.6 mm.

4.3 LENGTH OF THE OUTDOOR END :

According to the recommendation of IEC 137, the specific creepage distance should be in the range of 1.6 to 2.3 cm/kv depending on the atmospheric pollution level. A central value of 2.06 Cm/KV was selected. This value also conforms with that used by Siemens in their designs [2].

Total creepage distance required for 750 KV in air is 750 x 2.06 cm. The ratio of overall length to the creepage

distance of typical porcelain enclosure [2]

$$= \frac{1229}{2226}$$

∴ Length of the ourdoor end

$$= (750 \times 2.06) \times 1229/2226$$

$$= 837.95 \text{ cm.}$$

4.4 LENGTH OF THE IMMERSED END

For the bottom part of the bushing which is immersed in oil we take specific creepage distance half of that in clean air [6-5] and the ratio of length to the creepage distance is same as for the outdoor end.

The specific creepage distance in clean air was taken as 1.07 cm/KV [2]. So that the total creepage distance required for 750 KV/under oil is $750 \times \frac{1.07}{2}$ cm

∴ Length of immersed end $= (750 \times \frac{1.07}{2}.) \times \frac{1229}{2226}$

$$= 217.62 \text{ cm.}$$

So tha total length of the busing

$$= 837.95 + 217.62$$

$$= 1055.57 \text{ cm.}$$

4.5 MINIMUM THICKNESS OF CONDENSER INSULATION:

The thickness of commercially available paper is usually 0.005 inch [6-1]. From manufacturing considerations, the minimum number of layers in one condenser is 12. [6-1].

So the total minimum thickness of condenser insulation is 0.06 inch (0.1524 cm).

4.6 NUMBER OF CONDENSERS :

The potential difference across the first condenser

$$v_1 = E_{max} \, r \, \ln \left(\frac{r_1}{r} \right)$$

$$r = 2.06 \text{ cm (Section 4.2)}$$

$$r_1 = (2.06 + 0.1524) \text{ cm}$$

$$\therefore v_1 = 0.1470261 \, E_{max}. \text{ KV}$$

where E_{max} is the maximum radial electric field gradient allowable for paper insulation in KV/cm.

Highest system voltage for 750 KV bushing is 825 KV, which is taken as 10 % above the normal voltage (according to British practice [B-4])

So the no. of capacitor layers required $= \dfrac{825}{v_1}$

For Oil Impregnated paper insulation

$$E_{max} = 35 \text{ KV/cm for power frequency [B-4]}$$

which gives $v_1 = 0.1470261 \times 35$

$$= 5.1459 \text{ KV}$$

$\therefore$ Number of layers required $= \dfrac{825}{5.1459}$

$$= 160.32$$
$$\sim 161 \text{ layers.}$$

For condenser bushings, the radial impulse breakdown strengths are so large that they need not to be considered in the design and only power frequency voltages are involved in determining the radial gradients.

4.7 CONDENSER DIMENSIONS :

For ease in manufacture, it is better to have the same thickness of insulation in all the condensers. So, as a first approximation, the radius of Nth layer

$$r_N = (r + 1.524 \ N) \ mm$$

Using the criterion derived earlier, viz.,

$$r \ Lr_1 = r_1 \ Lr_2 = \ldots$$

length of the foil in the Nth condenser is

$$Lr_N = \frac{r}{r_{N-1}} \ Lr_1$$

4.8 ESTIMATION OF HOT-SPOT TEMPERATURE :

The equation derived in the earlier section was of an emperical nature in which the parameters in the expression of hot spot temperature were derived from experimentally measured values of temperature. In what follows, the problem has been approached from the very basic considerations, making use of published values of thermal conductivity to calculate the thermal resistances of different sections. The same boundary temperatures have however been retained as we donot have the heat run data for 750 KV bushing.

The bushing cross section is shown in Fig. (14).
The total bushing has been considered in two sections,
one above the flange and other below. The thermal model
is the same simple model shown in Fig. (11).

For the section above the flange we calculate the
thermal resistance of each horizontal strip separately as
shown in Fig. (15). Using the formula

$$R_D = \frac{g}{2\pi \ell} \, \ell n \, \frac{r_0}{r_1}$$

where g = thermal resistivity in $^{\circ}$C-m/watt

ℓ = length of the strip in m

r_0 = outer radius

r_1 = inner radius

For the total resistance above the flange, we add
all these branches in parallel, whence we get the value
of G_A. We have not taken into account the thermal resistances
of porcelain shell and oil layer. The design has to be
altered eventually, once the shell size etc are decided.

In a similar manner, we calculate the thermal resistance
of paper insulation core below the flange to give us the
value of Go.

Assuming the hottest spot to be in the middle of the
bushing along the flange

$$G_T = \frac{KA}{\ell}$$

K = Thermal Conductivity

ℓ = Length of Conductor Path

A = Area of Crosssection of the
conductor.

10555.7 mm

Conductor

8379.5 mm

Paper
Insulation

822.29 mm

2659.86 mm

261 mm

2176.2 mm

Porcelain(air)

Oil

Flange

Porcelain(oil)
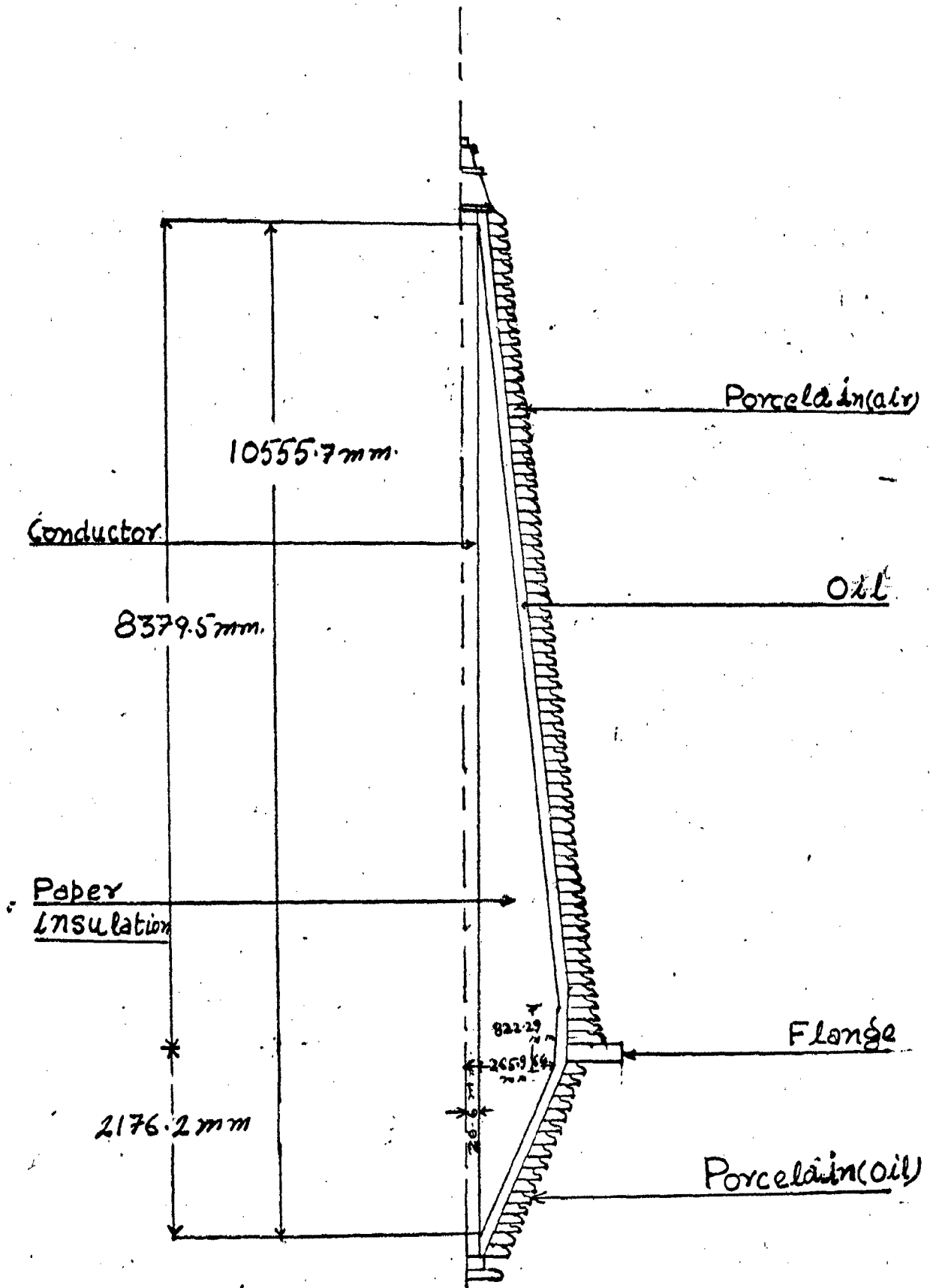
Fig.14 Main Dimensions of 750KV, 2000A, OIP,
        outdoor-immersed bushing

Equipotential cylinders

8379.5mm

10555.7mm

822.29 mm.

Flange

265.964mm.

20.6 mm

2176.2mm

Conducter
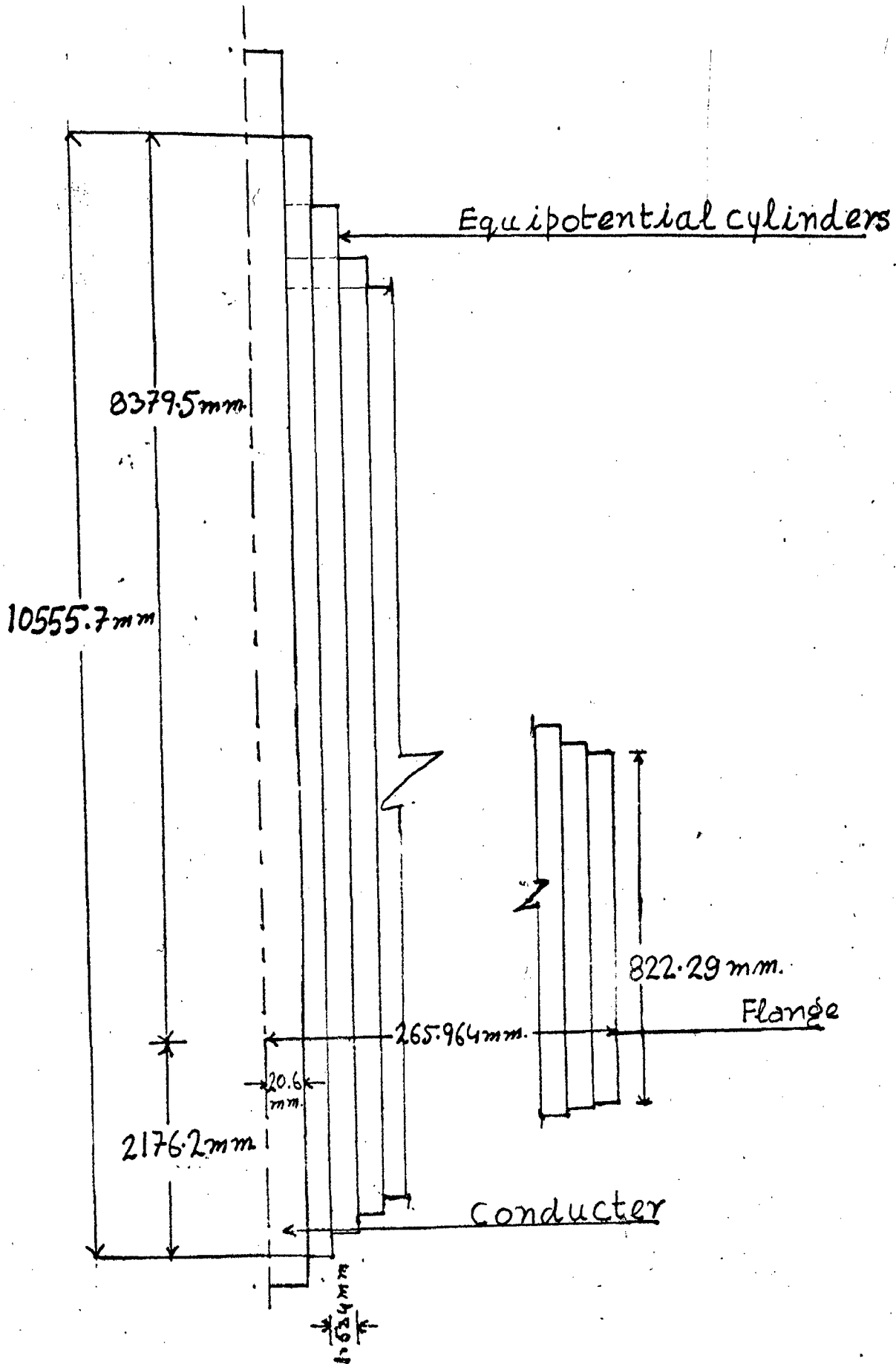
Fig. 15 Paper Insulation Core Consisting of '61 equipoten
layers of 750KV, 2000A, OIP, outdoor immersed Bushi

$K = 9.6 \times 0.393$ watt/cm-$^{\circ}$C for Copper

$\ell = 8.3795$ metre

$A = 1333.33$ mm^2

$$\therefore \; G_T = \frac{(9.6 \times 0.393 \times 10^2) \times (1333.33 \times 10^{-6})}{8.3795}$$

$$= 0.06 \text{ watt/}^{\circ}\text{C}$$

Similarly we can calculate G_B,

$$G_B = \frac{(9.6 \times 0.393 \times 10^2) \times (1333.33 \times 10^{-6})}{2.1762}$$

$$= 0.2312 \text{ watt/}^{\circ}\text{C.}$$

$$Q = I^2 R_c$$

$$= I^2 \left[1.1 \times \frac{p\ell}{A} \right]$$

$$= I^2 \left[1.1 \times \frac{0.01682 \times 10^{-6} \times 10.5557}{1333.33 \times 10^{-6}} \right]$$

$$= I^2 \left[1.46476 \times 10^{-4} \right] \text{ watt}$$

$$I \rightarrow \text{in amp.}$$

For rated current of 2000 Amp (1 p.u.)

$$Q = 585.91 \text{ watt}$$

Now the eq. for θ_{HS}

$$\theta_{HS} = \frac{Q + (G_0 + G_B)\,\theta_0 + G_T\theta_T + G_B\,\theta_B}{G_T + G_B + G_A + G_0}$$

If I is substituted in p.u the eq. becomes

$$\theta_{HS} = \frac{585.91\,I^2 + (G_0 + G_B)\theta_0 + G_T\theta_T + G_B\theta_B}{G_T + G_B + G_A + G_0}$$

4.9 VOLUME AND WEIGHT OF PAPER-INSULATION CORE :

For volume of paper insulation core, we calculate the volume of each condenser layer separately and then add them together to get the total volume of the insulation core.

For weight of the insulation core, we multiply the volume with the density of insulation and get the weight of insulation core.

After specifying the thickness of oil layer and porcelain shell, we can determine the total weight of the bushing.

4.10 THE COMPUTER PROGRAMME :

For designing the bushing, a computer programme was developed by the author [appendix(D)], which determines step by step the no. of layers, dimensions of layers, the thermal conductances of bushing below and above the flange and the volume of insulation core. In this programme, we design the condenser bushings for Oil Impregnated Paper. Synthetic Resin Bonded Paper and Completely Oil filled with mettalic cy-linder type equipotentials and compare the external dimensions, hot spot temperatures and weight of insulation cores.

5.0 RESULTS AND DISCUSSIONS

5.1 BUSHING DESIGN BASED ON RADIAL STRESS GRADING :

The computer programme described briefly in the previous section gives the following results.

(i) The outer radius of bushing insulation core.

For O.I.P bushing   = 265.964 mm

S.R.B.P. bushing   = 448.844 mm

Oil-filled bushing = 592.100 mm

(ii) The Thermal conductances G_A and G_O from the computer results are,

For O.I.P. Bushing

G_A = 24.775043 watt/^{O}C

G_O = 6.4341809 watt/^{O}C

For S.R.B.P. bushing

G_A = 24.739258 watt/^{O}C

G_O = 6.4248877 watt/^{O}C

For Oil filled bushing

G_A = 24189.555 Watt/^{O}C

G_O = 6282.1284 watt/^{O}C

Putting these values and values of G_T and G_B calculated previously in the expression for θ_{HS} (Section 4.8), we get the following expressions.

For OIP busing

$$\theta_{HS} = 18.600 \ I^2 + 0.2116 \ \theta_O + 1.905 \times 10^{-3} \ \theta_T$$
$$+ 7.34 \times 10^{-3} \ \theta_B$$

For SRBP bushing

$$\theta_{HS} = 18.627 \; I^2 + 0.2116 \; \theta_o + 1.907 \times 10^{-3} \; \theta_T$$
$$+ 7.35 \times 10^{-3} \; \theta_B$$

For Oil-filled bushing

$$\theta_{HS} = 0.01923 \; I^2 + 0.2062 \; \theta_o + 1.97 \times 10^{-6} \; \theta_T$$
$$+ 7.59 \times 10^{-6} \; \theta_B$$

For $I = 1.6$ p.u., from table 2 (observation E2), the boundary temperatures are

θ_o	θ_T	θ_B	θ_A	All are in
62	58	20	32	^oC above ambient

Using these values, the hot spot temperature of bushings while carrying a current of 1.6 pu. are

For OIP bushing $\qquad \theta_{HS} = 60.99 ^oC$

SRBP bushing $\qquad \theta_{HS} = 61.06 ^oC$

Oil-filled bushing $\qquad \theta_{HS} = 12.84 ^oC$

.All these values of θ_{HS} are above the ambient temperature.

(iii) The total volume of internal insulation for different bushing is as follows:

For OIP bushing $\qquad = 0.33793160 \times 10^9 \; mm^3$

SRBP Busing $\qquad = 0.58834028 \times 10^9 \; mm^3$

Oil-filled bushing $= 0.78435480 \times 10^9 \; mm^3$

Taking the specific densities for OIP, SRBP and Oil 1.30, 1.25 and 0.88 respectively, we get the approximate weight for internal insulation core.

for OIP busing   = 439.311 Kg.

SRBP bushing   = 735.425 Kg.

Oil-filled busing = 690.232 Kg.

These results are put in table (4) for comparision.

Table -3

CHARACTERSTICS OF DIFFERENT BUSHING INSULATION SYSTEMS

Characterstics	OIP	SRBP	Oil-filled
Emax KV/cm	35	20	15
Thermal resistivity $^{\circ}$C-m/watt	6	6	0.0061275
Specific density	1.30	1.25	0.88

Table -4

COMPARISION OF DIFFERENT BUSING TYPES

Parameters	OIP	SRBP	Oil-filled
Outer radius of insulation core (mm)	265.964	448.844	592.100
Hot spot temp. above ambient ($^{\circ}$C)	60.99	61.06	12.84
Approx.weight (Kg.)	439.311	735.425	690.232

From the above table (4) we see that the oil
impregnated paper bushing is best for 750 KV range as
it possesses least radius and weight. The hot spot
temperature is higher in comparision to oil-filled type but
this is well within the permissible operating temperature
for this class of insulation viz. $70^\circ C$ above ambient.
This type of bushing will have uniform radial grading
but axial stresses will not be uniform.

5.2 BUSHING DESIGN BASED ON AXIAL STRESS GRADING :

For this, we shall select the dimensions of layers
in such a way as to make the distribution of field intensity
in the axial direction uniform. For this we shall take the
lengths of projections equal i.e. $Lr_2 - Lr_1 = Lr_3 - Lr_2 = \ldots$
and so on and we shall select the radii of the layers r_1 and
r_2 such that the capacitances of all layers are equal. But
this is only the approximate method for grading of axial
stresses. For exact method, the creepage distance between
the edges of two consecutive metal foils should be same
throughout the insulation core. Then, only the axial stresses
will be uniformly graduated throughout the insulation core.

(a)   For approximate method, we divide the total overhang equally
between the different condensers and in this way, calculate the
length of different layers.

After calculating the length we calculate the radii
of all layers in such a manner that the capacitances of

each and every condenser is equal.

$$\frac{Lr_1}{\ln(\frac{r_1}{r})} = \frac{Lr_2}{\ln(\frac{r_2}{r_1})} = \ \ldots\ldots$$

From this expression it is evident that the thickness of the condenser, $r_n - r_{n-1}$, will go on increasing towards the flange, thus leading to increasing creepage distances, so we can achieve only the nearly uniform axial grading.

(b) For exact method, we assume the thickness of first condenser to be equal to minimum thickness prescribed for capacitor layers based on manufacturing consideration and the length to be equal to the bushing length. We fix the creepage distance required between the edges of successive metal foils by choosing proper specific creepage distance. We can then get the minimum overhang which is equal to the creepage distance required minus the thickness of first layer. However, we allow a slightly higher overhang on the outdoor side in order to make up for the extra bushing length required above the flange. Then $Lr_2 = Lr_1 -$ total overhang. After getting the length of second layer (Lr_2) we can calculate (r_2) by the above equation. In this way we can calculate the position and length of each condenser throughout the insulation core.

For this method, we choose the specific creepage distance 0.52 cm/KV, so the minimum creepage distance required will be $(5.2 \times \Delta V)$ mm.

In both these methods (a) and (b), the thickness of different condenser layers are different. But we round off the thickness to the multiples of 0.127 mm which is thickness of one paper layer so that each condenser is composed of a whole number of layers, viz. 12, 13,14 and so on, where 12 is the minimum number of paper layers in one condenser.

Two computer programmes given in appendix (E) and (F) have been developed which gives the following results for OIP bushing.

(i) approximate method (appendix E).

Outer radius = 6916.446 mm

Weight of insulation core = 538002.6 kg.

(ii) Exact Method (appendix F)

Outer radius = 2410.613 mm

Weight of insulation Core = 52841.13 kg.

From the results based on uniform axial grading of bushing, we see that firstly the dimensions of bushing become very large and secondly, the radial stresses will also not be uniform, so it is better to base the design on uniform radial grading which also provides a compact design.

5.3 AXIAL STRESSES IN THE DESIGN BASED ON UNIFORM RADIAL GRADING :

As we are putting the capacitor layers around the central conductor lengthwise in the same ratio as that of

outdoor and immersed end of bushing, the axial stresses
will be more in the immersed part. The minimum creepage
distance required between ends of two metal foils for
OIP bushing (specific creepage distance = 0.52 cm/KV)
will be (0.52 X 5.1459) cm or 2.67 cm, where 5.1459 KV
is the voltage of each condenser. The overhand on the
outside end will be proportionately more to account for
the increased outside length. Thus the total overhang
required for adequate design free of all possible
flashovers between metal foils will be

$$= \frac{1055.57}{217.62} \text{ X } [\ 0.52 \text{ x } 5.1459 - .1524]$$

where 0.1524 cm is the thickness of insulation.

Thus total overhang   = 12.24 cm

        = 122.4 mm

In our proposed design of radially graded OIP bushing
which has 161 layers, after 22 layers, creepage distance
between adjacent metal foils becomes less than minimum
and bushing may have flashovers in very adverse conditions.
We could remedy this situation by coating the exposed edges
of metal foils by some insulating medium of higher
dielectric strength. Alternatively we could let the
insulation between two metal foils project out in order
to increase the creepage distance. These arrangements will
affect the heat dissipation from busing to some extent
in the region beyond the 22nd condenser because the metal
foils are not exposed to the surrounding oil. But this

may not be very significant since much of the bushing heat
is conducted to the oil by the condensers before the 22nd
which are more near to the hot spot.

By these arrangements, we can have a near perfect
bushing having uniform radial grading, free from all
flashovers between metal foils, thermally stable and of
very compact size. The oil and porcelain clearances will
be decided by manufacturers depending upon the size and weight
of internal insulation core and required specifications of
the bushing.

———

6.0 CONCLUSIONS :

(i) The design based on radial field grading resulted in a bushing of smaller diameter in comparison to the design based on axial field grading. With radial grading, however, the creepage distance between equipotentials was found to be insufficient after the 22nd equipotential. It is proposed to overcome this difficulty by either projecting out the insulation between two equipotentials or by coating the exposed edges of the metal foils by an insulation of higher dielectric strength. This is not expected to upset the thermal performance to a large extent.

(ii) Three types of bushings were designed viz. OIP, SRBP and Oil-filled and among them OIP bushing was found to be the best suited for this voltage range.

(iii) No account has been taken of the external porcelain housing in the calculations of hot spot temperature. The main difficulty was in selecting the wall thickness. This information could not be obtained from Porcelain manufactures in this country, even after supplying the details of external profile etc. Once this information is available, we can

have the better estimation of hot spot
temperature.

(iv) The characterstics of the bushing designed
conforms generally with those of existing
designs of ehv bushing.

7.0   SUGGESTIONS FOR FUTURE WORK :

One immediate possibility is to construct a model condenser in our HV laboratory and test it for internal discharge and RI performance. This is possible with the available h.v test sources.

REFERENCES

1. Yamamoto, Kagaya, Kojima and Kawai-EHV Elephant Type
   Bushing, J.IEEE (Power Apparatus and Systems), Vol.68,
   No.10, October 1963, pp. 698-705.

2. Beknke, C and Potter C., New 110KV Condenser Wall Bushing,
   Discription, Siemen's Review (Germany) Vol.34, No.5,
   (May 67), pp. 192-4.

3. KAPPELER, HANS. Resin bonded bushings for EHV systems,
   J. IEEE (Power Apparatus and Systems), Vol.87, No.2,
   Feb. 68, pp.394-9.

4. McNutt, W.J. and Easley, J.K., Mathematical Modelling-
   A basis for bushing loading guides, J IEEE (Power
   Apparatus and Systems), Vol. 97, No.6, Nov/Dec.1978
   pp. 2393-2404.

5. Herbert, P.P. and Steed, R.C., A High Voltage Bushing Thermal
   Performance Computer Model, JIEEE (Power Apparatus and
   Systems), Vol.97, No.6, Nov/Dec.1978, pp. 2219-2224.

6. Hammer, Dr. F. and Kirch, H.J.-Design, manufacture and
   testing of RIP bushings and the special application as
   components of SF_6 insulated H.V.equipments, J.Electrical
   India, Vol. 19, No.4, 28th Feb. 1979, pp. 21-2, 25-9.

7. Prasad, N.M. - Condenser Bushing, J.Electrical India,
   Vol.20, No.4, 29th Feb., 1980, pp. 21-3

B-1 Transformer Construction and Operation, Emerson
G.Reed, Mcgraw-hill Book Company, Inc.(1928), pp.91-98.

B-2 Electric Power Equipment, J.G.Tarboux, Mcgraw-Hill Book
Company, INC (1946), pp. 198-199.

B-3 Discharge Detection In High Voltage Equipment,
F.H.KREUGER, Tempe Press Books Ltd., LONDON (1964),
pp. 47-71.

B-4 High Voltage Technology, L.L.Alston Oxford University
Press (1968), pp. 228-253.

B-5 High voltage Engineering, M.P.Chourasia, Khanna Publishers,
Delhi (1980), pp. 198-212.

B-6 Transformer, Kenneth L.Gebert and Kenneth R.Edwards,
American Technical Society (1980), pp. 199-200.

BIBLIOGRAPHY

1. Linderholm, S., Transformer for 750 KV, J ASEA, Vol. 35, No.4, 1962, pp. 55-7

2. Piotrowski, J. and Winiarski, J., 110KV SF_6-Air Bushing, Pr. Inst. Elektrotech (Poland), Vol.26, No.105,1978,pp.119-22

3. Cradhead, D.O. and Easley, J.K., Thermal test performance of a modern apparatus bushing, J.IEEE (Power Apparatus and systems) Vol.97, No.6, Nov/Dec.1978, pp. 2291-9.

4. Marconcini, A and Villa, G. The autotransformer for 1000KV Project- The bushings, Electtrotechica (Italy), Vol.66, No.10, Oct. 1979, pp. 832-9.

5. Peshehke, E.F., Cable bushing in metal-enclosed SF_6 insulated high voltage switching installations, Elektrizitaetswirtschaft (Germany), Vol. 78, No.26, (21 Dec. 1979), pp. 1060-4.

6. Rachui, R.A., Strain Relief bushings for Cables, IBM Tech. Disclosure Bull (USA) Vol.23, no.7B, (Dec. 1980), p. 3075.

7. Yamagiwa, T., Kamata, Y., and Yoshioka, Y., Dielectric characterstics of gas insulated bushings in air-dry and wet conditions, J. IEEE (Power Apparatus and Systems),USA, Vol. PAS-100, No.6, (June 1981), pp.2746-51.

8. Linderholm, S., Capacitance graded bushings with insulation of oil impregnated paper, ASEA J. (Sweden), Vol. 54, No.4, pp. 79-84, 1981.

9. Quirk, J.F., Janocka, M.A. and Shestak, E.J., High Voltage-high current cryogenic bushing, J.IEEE (Power Apparatus and Systems), Vol.100, 1981, pp. 281-4.

10. Saita, S., Inagaki, K., Sato, T., Inni, Y. and
    Okuyama, K., Eddy currents in structure surrounding
    large current bushings of a large capacity
    transformer, JIEEE (Power App. and Systems), USA,
    Vol. PAS-100, No. 11 (Nov.81), pp. 4502-9.

11. Knyazer, K.A. 500 KV Transformers, Energetik (USSR),
    Vol.14, No.12, (Dec. 1966), pp. 23-4.

12. Rohrbach, F., H.V.Electrostatic separators Design,
    Vide (France) Vol. 212, (Jan-Feb. 1966), PP. 52-74.

13. Krasser, G., H.V.Transformer Bushing, Thermal Problems
    Calculations, Bull Assoc. Suisse Elect. (Switzerland),
    Vol. 58, No.7, (Feb.68), pp. 394-9.

APPENDIX A

TESTING OF BUSHINGS

A work on high-voltage bushing would not be complete without some reference to the tests imposed on them to prove the designs and quality of manufacture. Tests may be specified as type tests i.e. tests intended to prove design features of bushings, or as routine tests which check the quality of individual bushings. Some tests may have a dual purpose and can serve as either type tests or routine tests according to circumstances.

Tests to check the dielectric, thermal and mechanical properties of bushings comprise:

(1.0) Type Tests:

1.1 The wet power frequency voltage with stand test

1.2 The dry lightning impulse voltage with stand test

1.3 The switching impulse voltage withstand test

1.4 The thermal stability test

1.5 The measurement of radio interference

1.6 The temperature rise test.

(2.0) Routine Tests:

2.1 Measurement of the dielectric dissipation factor (tan δ.) and the capacitance at ambient temperature.

2.2 The dry power frequency voltage withstand test.

2.3 The measurement of partial discharge level.

2.4 The power frequency voltage withstand tests of the voltage tapping and test tapping insulation.

(2.5) Tests for leakage of internal filling.

(3.0) Special Tests:

(3.1) Test for leakage at the flange or other fixing device.

(3.2) The short time current test to be carried out as
agreed upon supplier and purchaser.

(3.3) Mechanical tests to be carried out as agreed upon between
supplier and purchaser.

Condition of bushings during the dielectric and thermal tests:

Dielectric and thermal tests shall be carried out only
on bushings complete with their flanges or other fixing devices
and all accessories with which they are fitted when in use,
but with protective gaps, if any, removed Test tappings and
voltage tappings shall either be earthed or held near earth
potential. Before the tests, the outside surfaces of the
insulating parts shall be carefully cleaned. Liquid filled
bushings shall be filled to the normal operating level with
the insulating liquid of the quality specified by the supplier.

For busings intended to be surrounded in operation by
a liquid or solid insulating medium other than oil, either
completely or partially that insulating medium shall be
replaced by oil for the dielectric and thermal tests, unless
otherwise stated.

For bushings intended to be surrounded in operation
by gaseous insulating medium other than air at atmospheric
pressure, either completely or partially, the gaseous
insulating medium shall be replaced by oil for the dielectric
routine and sample tests, unless otherwise stated. However,
for the dielectric and thermal type the gaseous insulating,
medium shall be as similar as possible to that used in normal
operation.

(1.0) Type Tests:

(1.1) Wet power frequency withstand test:

The test voltage duration is one minute to ten seconds
(usually of 30 s duration), with the bushing mounted as in
service under artificial rainfall of specified intensity and
water resistivity. The values of wet power frequency test
voltages are indicated in Table I.

(1.2) Dry Lightning impulse voltage withstand test:

During the dry lightning impulse voltage withstand
test, the bushing shall be subjected to five full wave impulses of
positive polarity and five full wave impulses of negative
polarity of the standard wave form 1.2/50 having the relevant
peak values of voltage in Table I, the voltage being applied
between the internal conductor and flange or other fixing
device.

If no flashover or puncture occurs, the bushing shall

be considered to have passed the test. If there is puncture

or more than one flashover, the bushing shall be considered

to have failed the test. If only one flashover occurs, a

further series of ten impulses shall be applied, with the

same polarity as that at which the flashover occured. If

during the course of these ten additional impulses no flashover or

puncture occurs, the bushing shall be considered to have passed

the test.

(1.3)Switching impulse voltage withstand test:

The switching impulse voltage withstand test will only be

made if agreed upon between punchaser and supplier.

This test is only applicable to bushings of rated voltage

equal to or above 300 KV.

(1.4)Thermal Stability test:

The thermal stability test is only applicable to bushings

of which the major insulation consists of organic material,

having a rated voltage equal to or greater than 145 KV and

intended for apparatus filled with an insulating medium the

operating temperature of which is between $60^{o}C$ and $100^{o}C$.

The bushing to be tested shall be installed under

conditions similar to those of normal operation. It shall not

carry current, unless otherwise agreed upon.

During the test, the oil shall be maintained at a temperature of $90 \pm 2^{\circ}$C. This temperature shall be measured by means of thermometres immersed in oil, 3 cm below the surface and 30 cm from the bushing.

During the test, tangent delta measurements shall be made by means of a Schering bridge, or equivalent method, at a voltage equal to U_N (Normal voltage) for bushings of which U_N is below 245 KV, and at a voltage equal to 0.7 U_N for bushings of which U_N is equal to or above 245 KV. For each measurement of tangent delta, the ambient air temperature shall be recorded.

The loss curve shall be plotted with the measured values of tangent delta as ordinates and times as abcissae.

The bushing tested has reached thermal stability when its losses remain sensibly constant for three hours.

Upon request of the purchaser, a detailed test report shall be furnished.

1.5 Measurement of radio interference:

The measurement of radio interference voltage (R.I.V) generated by a bushing is made solely to ensure that discharges originating at the bushing will not interfere unduly with the operation of radio equipment. It is not an alternative to partial discharge test which is concerned with limiting discharge internal to the bushing to a level at which its insulating properties will not be impaired.

A. (vi)

The test shall be made on request of the purchaser and the maximum permissible value of R.I.V. shall be agreed upon supplier and purchaser. In this test the protective gaps shall not be removed. Atmospheric conditions shall be recorded, the relative humidity shall not exceed 80 % .

The rated voltage (U_N) of the bushing shall be applied and reduced to the agreed test voltage at which the radio interference shall be measured. It is permissible practice to wipe the outside surfaces of the insulating parts with a dry lint-free cloth before the test and to condition the bushing at the rated voltage for two minutes. The measurements shall be made at a frequency of 1.0 MHz or 0.5 MHz $\pm$ 10 % using a measuring set conforming with C.I.S.P.R. publication 1.

(1.6) <u>Temperature rise test:</u>

This test is applicable to all bushings. However, on bushings, the major insulation of which consists of an inorganic material, this test is carried out only on request of the purchaser.

The permissible limits of temperature rise are given below.

(a) for indoor, outdoor, outdoor-indoor bushing

- 50° C above the ambient air temperature.

(b) for indoor-immersed and outdoor immersed bushings of which the maximum temperature for the immersion medium is 55°C above ambient air temperature - 20°C above the temperature of the immersion medium.

(c) for completely immersed bushing - 20°C above. the temperature of immersion medium

Upon request of the purchaser, a detailed test report shall be furnished. The temperature rise test may be omitted if the supplier can demonstrate by any other means (e.g. test result of comparable bushings) that the specified temperature rise limits will be met.

(2.0)Routine Tests:

(2.1)Measurement of the dielectric dissipation factor (tan δ) and the capacitance at ambient temperature :

The measurement of the dielectric dissipation factor (tan δ) and the capacitance at ambient temperature is applicable to all condenser bushings and non condensor bushings of cast insulation type.

During this test, the bushing conductor shall not carry current.

The ambient temperature and the temperature ofthe immersion medium, if any, shall be between 10°C and 40°C.

The measurement of the dielectric dissipation factor (tan δ) shall be made as a function of voltage by means of Schering bridge or other equivalent method at and between the limits 0.3 U_N - 1.0 U_N.

The maximum values of the tangent delta, measured at U_N for U_N < 52 KV and 0.3 U_N for U_N ≥ 52 KV are as follows:

(a) Condensor bushings:

For resin impregnated paper, resin bonded paper,

Cast insulation, composite   - 0.015

for oil impregnated paper   - 0.007

(b) Non Condensor bushings

For cast insulation   - 0.020

The capacitance of the bushings is to be measured at approximately 0.6 U_N, before and after each series of dielectric and thermal tests. The capacitance measured at the end of series of tests should not differ by more than 1 % from that measured at the beginning of the series of tests.

(2.2) Dry power frequency withstand test:-

This test is applicable to all bushings. The test duration is one minute. The values of the dry power frequency test voltage are indicated in Table -I.

(2.3) Measurement of partial discharge level :

The measurement of the partial discharge level shall follow all other type, routine and special tests. However, as long as it is not definitely known that discharge magnitude causes a dangerous deteroriation of the type of insulation concerned, this test is still of a tentative nature and, therefore, is only carried out as an acceptance test upon request of the purchaser.

This test is not applicable to bushings the major insulation of which consists of inorganic material or to those the maximum dielectric stress of which is below

1.5 KV (r.m.s)/mm at a voltage which is equal to $U_N/\sqrt{3}$. The supplier must give proof that this maximum dielectric stress is not exceeded.

Different standard test circuits are used for partial discharge measurements. The elements of the test circuit should be chosen such that the value of the minimum measurable discharge level shall be at least 5×10^{-12} C when measuring the apparent charge or at least 10^{-20} C^2/s when measuring the quadratic rate.

The partial discharge level shall be measured at U_N and at 0.63 U_N. Before making the measurements the test voltage is raised to U_N and held constant for one minute. The first measurement is then made and the test voltage is subsequently reduced to 0.63 U_N, at which value the second measurement is made immediately.

Practical experience has shown that the following approximate values of the partial discharge level with reference to the terminals of the bushing, measured at 0.63U_N, seem to be acceptable:

Type of bushing	Discharge magnitude (c)	Quadratic rate (c^2/s)
G.I.P. condenser bushing.	10×10^{-12}	10^{-20}
Resin bonded paper condenser bushing with metallic conducting layers.	100×10^{-12}	10^{-16}
Resin bonded paper condenser bushing with non-metallic conducting layers.	100×10^{-12}	10^{-18}
Resin impregnated paper bushing	20×10^{-12}	5×10^{-20}
Cast insulation bushing	20×10^{-12}	5×10^{-20}

The relationship between the values of quadratic rate is only an approximate one and depends on the type of material.

In the case of bushings of rated voltage equal to or above 245 KV, it is recommended not to consider the two measuring points mentioned above sufficient but to plot the the whole curve showing the partial discharge levels with ascending and descending, voltage between 0 and U_N.

(2.4)Power Frequency Voltage Withstand Test of Test and Voltage Tappings insulation :

This test is applicable to all tapping. The duration of the test voltage is one minute. The values of test voltage are as follows:

A.(xi)

- test tapping　　　　: 2 KV

- voltage tapping　　　: Three times the rated
　　　　　　　　　　　　 voltage of the voltage
　　　　　　　　　　　　 tapping.

(2.5) Test for leakage of internal filling :

The test for leakage of internal filling is only
applicable to liquid filled bushings. Two alternative test
procedures may be used at the choice of the supplier.

a. Test with oil or insulating liquid at air temperature.

b. Test with compressed gas.

(3.0) Special Tests :

(3.1) Test for leakage at flange or other fixing device :

The test for leakage at flange or other fixing device
is only made on request of the purchaser and upon an agreed
number of bushings.

This test is applicable to indoor-immersed, outdoor
immersed and completely immersed bushings. The two alternative
test procedures given below may be used at the choice of the
supplier.

(a) Test with oil at ambient temperature :

The bushing, complete as for normal operation, shall
be mounted on a tank filled with transformer oil at ambient
temperature.

A pressure of 1 $\pm$ 0.1 bar above the atmospheric pressure
shall be produced inside the tank. The pressure shall be
maintained for at least 12 h.

A.(xii)

The test shall be considered satisfactory if there is no evidence of leakage of oil.

(b) Test with compressed gas:

The bushing, complete as for normal operation, shall be mounted on a tank filled with air or any suitable gas maintained at a pressure of 1 ± 0.1 bar above the atmospheric pressure. The duration of test shall be 15 min. The test shall be considered satisfactory if there is no leakage of oil.

3.2 The short time current test to be carried out as agreed upon supplier and purchaser.

3.3 Mechanical tests to be carried out as agreed upon between supplier and purchaser.

Table I

TABLE I(A) (for rated voltages equal to or below 52kV)

Rated voltage U_N KV (rms)	Power frequency withstand voltage KV (rms) [dry and Wet]	Dry lightning impulse withstand voltage 1.2/50 KV (peak)
3.6	21	45
7.2	27	60
12	35	75
17.5	45	95
24	55	125
36	75	170
52	105	250

TABLE IB (For rated voltages equal to or above 72.5 KV)

Rated voltage U_N KV(rms)	Power frequency withstand voltage dry and wet KV (r.m.s)	Dry lightning impulse withstand voltage 1.2/50 KV (peak)	Switching impulse withstand voltage KV (peak)
72.5	140	325	
123	185	450	
	230	550	
145	185	450	
	230	550	
	275	650	
170	230	550	
	275	650	
	325	750	
245	325	750	
	360	825	
	395	900	
	460	1050	
300	395	900	...
	460	1050	...
	510	1175	...
362	460	1050	...
	510	1175	...
	570	1300	...
420	570	1300	...
	630	1425	...
	680	1550	...
	740	1675	...
525	630	1425	...
	680	1550	...
	740	1675	...
	790	1880	...
765	...	...	...
	...	...	...
	...	...	...

Notes :   1. The underlined values are full insulation

values.

2. For rated voltages of 300 KV and above on full

insulation values are indicated since
full insulation is not considered applicable

to such systems.

APPENDIX -B

B.1 OPERATING CONDITIONS OF BUSHINGS:

Operating conditions of bushing as specified by International Electrotechnical Commission [IEC] are as follows:

(i) Altitude: -

Unless otherwise stated, it shall be assumed the bushings of which one or both ends are intended to be in air at atmospheric pressure are designed for operation at altitudes not exceeding 1000 metres.

The amount by which the insulation level, on which the air clearance is based should be increased is, for general guidance, 1.25 % for each 100 metres in excess of 1000 metres above sea level.

(ii) Temperature of the Cooling media :-

Unless otherwise stated, it shall be assumed that bushings are designed for operation at temperatures (in $^\circ$C) of the cooling media not exceeding the following limits:

- ambient air: maximum 40°C

                  maximum daily mean 30°C

                  for indoor bushings:

                         Class 1 : minimum $- 5^\circ$C

                         Class 2 : minimum -20°C

                         Class 3 : minimum -40°C

B.(ii)

for outdoor bushings:

Class 1 : minimum -25° C

Class 2 : minimum -40° C

Class 3 : minimum -60° C

- immersion medium :

maximum -100°C

daily mean -90°C

Notes

(a) The above values for immersion medium are to be used in the absence of other information.

(b) The mean temperature of the cooling medium may be calculated by averaging 24 consecutive hourly readings. If the ambient air is the cooling medium, the average of the maximum and minimum daily temperatures may be used. The value which is obtained in this manner is usually slightly higher than the true daily average but does not differ from it by more than 1°C.

(iii) Angle of mounting:

Unless otherwise stated it shall be assumed that the bushing is designed for mounting at any angle of inclination not exceeding 30° from the vertical.

(iv) Exposed and non-exposed installations :

Unless otherwise stated, it shall be assumed that the bushing is designed for operation in exposed installations.

(v) <u>Minimum values of Creepage distance</u> :

The minimum values of creepage distance (in mm per unit of rated voltage) for bushings one or both ends of which are intended to be outdoor are the following:

- for normal and lightly   : 16 mm/KV
  pollued atmospheres

- for heavily polluted atmosphere: 23 mm/KV

(vi) <u>Limits of temperature rise:</u>

Bushings shall be designed in such a way as to ensure that in continuous operation, at rated current and frequency the temperature rise of the hottest spot of the current carrying parts:

- in the case of bushing with an integral conductor, measured on the conductor and other current carrying parts.

- in the case of a busing with a conductor drawn into the central tube, measured on the conductor, central tube and other current carrying parts,
  does not exceed the limits specified below:

(a) for indoor, outdoor and outdoor-indoor bushings — $50^{\circ}C$ above the ambient air temperature.

(b) for indoor-immersed and outdoor- immersed bushings, of which the maximum temperature for the immersion medium is $55^{\circ}C$ above the ambient air temperature. — $20^{\circ}C$ above the temperature of the immersion medium.

(c) for completely immersed   20°C above the
    bushings   temperature of the immersion
                                  medium.

Alternatively, when the busing is supplied as an
integral part of the switchgear or similar apparatus, the
thermal performance shall be such that it will meet the
thermal requirements for the apparatus as demonstrated
by the temperature rise test on the complete apparatus with
the bushing fitted, when such a test is carried out

B.2 Information to be furnished when Ordering and Markings

Enumeration of Characterstics:

When specifying bushings, the purchaser should
furnish as much of the following information as necessary
to determine clearly the required characterstics.

1.   Application :

Application including the type of apparatus for which
the bushings are intended and the corresponding IEC apparatus
recommendation.

2.   Classification :

The Type of bushing for e.g. outdoor, indoor, outdoor-
indoor, indoor- immersed, outdoor- immersed or completely
immersed.

3.   Ratings :

3.1   Rated voltage
3.2   Rated phase to ground voltage

3.3 Insulation level.

3.4 Duration of wet power frequency voltage withstand level - 10s or 60s.

3.5 Rated current

3.6 Rated short time current, if deviated from 25 times rated current.

3.7 Duration of short time current, if deviating from one second.

3.8 Rated frequency

4. **Operating Conditions**

4.1 Altitude, if exceeding 1000 metres. In this case, state also if normal air clearances are accepted or if increased insulation level is required.

4.2 Class of minimum ambient air temperature.

4.3 Immersion medium.

4.4 Minimum level of immersion medium.

4.5 Maximum external operating pressure.

4.6 Angle of mounting

4.7 Normal, lightly or heavily polluted atmosphere.

4.8 For bushings subject to mechanical forces in operation, the magnitude, direction and nature of these forces.

5. **Design**

5.1 For bushings supplied without a conductor, diameter and position of the conductor with which the bushing will be fitted in operation.

5.2 Particular dimension requirements, if any

5.3 Test tapping or voltage tapping, if required.

5.4 The length of the earthed sleeve located next to the flange or other fixing device if one or more current transformers to be installed.

5.5 General information concerning the position of the bushing in relation to the earthed parts of the apparatus for which the bushing is intended.

5.6 Whether protective gaps are fitted or not.

Markings

All bushings shall carry markings which correspond to the types of bushings specified under two sub-classes as follows:

1. Condenser bushings

1.1 Supplier's name or mark, year of manufacture and serial number.

1.2 Rated voltage and rated phase-to-ground voltage.

1.3 Insulation level, rated current, rated frequency.

1.4 Maximum permissible angle of inclination, if exceeding 30° from the verticle.

1.5 Mass, if above 100 Kg.

Example: Supplier's Mark

19.. XXX/245-142-1050-460KV/400A/50~/45°/360 Kg.

2. All other bushings

   2.1 Suppliers name or mark

   2.2 Type

   2.3 Rated voltage and rated phase to ground
      voltage.

   2.4 Rated current

   2.5 Mass, if above 100 Kg.

APPENDIX-C
DETECTION OF DISCHARGES

Detection comprises the determination of the absence
or presence of discharges. The voltage at which the dis-
charges appear is determined. The magnitude of the discharges
may be measured by means of several electrical methods. The
choice of the method for location of discharge depends
strongly on the nature of the investigated object. But even
if the magnitude and location of the discharges and
characterstics such as field strength and frequency are
known, it is difficult to predict the voltage life of the
dielectric.

Electrical Detection:

Principle: The discharges in a sample cause current
impulses in the leads of the sample. A great variety of
circuits is in use to detect these impulses , but all these
circuits can be reduced to one basic diagram (Fig.I). The
elements are High voltage source, sample a affected by
discharges, Impedance Z across which voltage impulses occur
caused by the current impulses in the sample. Coupling capa-
citor K, which facilitates the passage of the high frequency
current impulses.

Amplifier A

Observation unit O which may be for instance a loudspeaker,
a voltmeter, or an oscilloscope. Some of these elements
are discussed in more detail in following discription.

The detection impedance:

The impedence Z may be connected in two ways: either Z placed in series with the sample or Z is placed in series with the coupling capacitor which is indicated in Fig. I by a dotted line. Both ways are electrically equal: the same voltage occurs across the impedance Z (assuming that the impedance of h.v source is large). In practice the connection of Z may be of importance. For instance, if the sample is large, Z is often placed in series with K so that the large charging current of a does not pass through the impedance Z. Two impedences commonly used are a resistor R shunted by a parasitic capacity C, or an oscillatory circuit, LCR. The voltage impulses which occur across these impedances may be calculated with the aid of laplace transformation.

RC Circuit: —

In the RC circuit the impulse appears to be uni-directional of shape as shown in Fig. II. The impulse is given by

$$V = \frac{q}{(1+C/K) \; a+o} \; e^{-t/R_m} \qquad \qquad ...(1)$$

where q is the magnitude of the discharge causing the impulse q = b ΔV.

Furthermore $\qquad m = \dfrac{ak}{a+k} + c$

LCR circuit: (Fig. III)

In case of the oscillatory LCR circuit, the impulse is an attenuated oscillation with the same crest voltage as with an RC circuit.
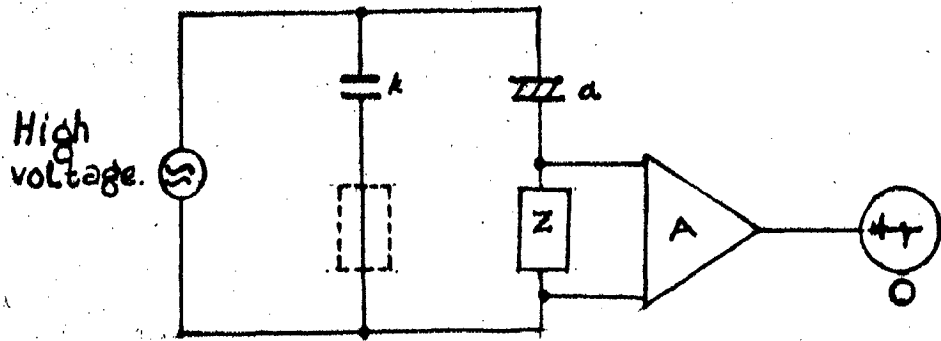
fig I:-Basic diagram for electrical
discharge detection
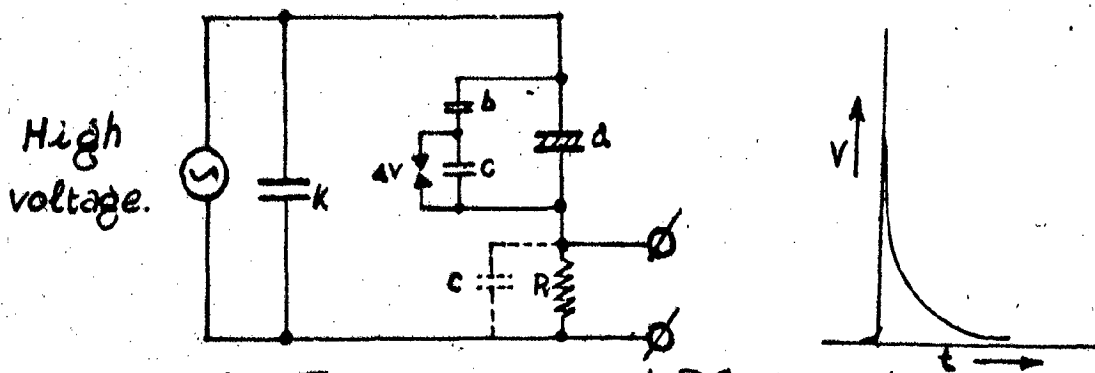
fig.II:- Respons with R.C.circuit.
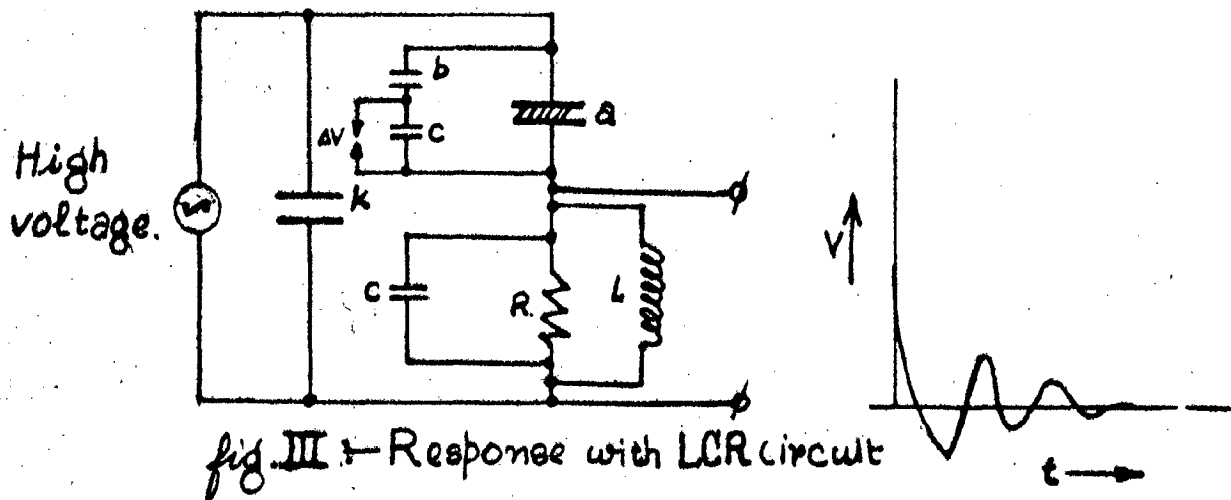
fig.III :- Response with LCR circuit

C.(iii)

$$V = \frac{q}{(1+c/k)a+c} e^{(-t/2R_m)} \cos wt \qquad ...(2)$$

where,

$$w = \sqrt{\frac{1}{L_m} - \frac{1}{4R^2_m{}^2}}$$

and m is same as above.

From the above we conclude

i.   The height of the impulse is proportional to the
magnitude q of the discharge.

ii.   The height of the impulse is independent of R. However, if
R is small the time constant R_m is small and thus the
impulse is sharp. In most amplifiers this sharp impulse
will not fully be amplified and the resulting impulse

becomes smaller if R is decreased.

iii. If a is large the height of the impulse is determined
by 'a' only, as

$$v \simeq \frac{q}{a}, \text{ for a} \gg C \text{ and k.}$$

iv.   It follows from Eq. (1) that a coupling capacitor k
is necessary, as otherwise c/k in the denominator is
large and the impulse becomes small.

Frequency spectrum- choice of amplifier :

After RC circuit : The unipolar impulses produced over the
RC detection impedance have a frequency spectrum which is
nearly constant in height up to a frequency $f_1 = 1/(2\pi R_m)$,
as shown in Fig. IV. As m depends on the circuit constants

(m=[a k]/[a+k] + c) the extension of the frequency
spectrum depends on the circuit and the magnitude of
the resistor R.

The amplifier used for amplification of these
impulses should obviously have a bandwidth which extends
to or beyond f_1. In some cases a narrow band amplifier
with a midband frequency below f_1 is used, as shown
under A in Fig. IV. The height of the signal obtained is
proportional to that of the original signal.

After LCR Circuit :

The oscillatory impulses which occur over an LCR network
have a frequency spectrum as shown in Fig. (V). The midband
frequency w is given by Eq. (2), it follows from this formula
that w is determined both by the LCR impedence and the
circuit constants.

The amplifier behind an LCR network should have a band
width which is equal to or broader than that of the signal.
According to 'Mole' sufficient sensitivity is obtained if
this bandwidth is more than thirty times the bandwidth of
the signal. If the sample comprises self induction, as is
the case, for instance, in a transformer, the frequency
spectrum is not smooth. In such a case RC detection with
a broad-band amplifier is preferred.
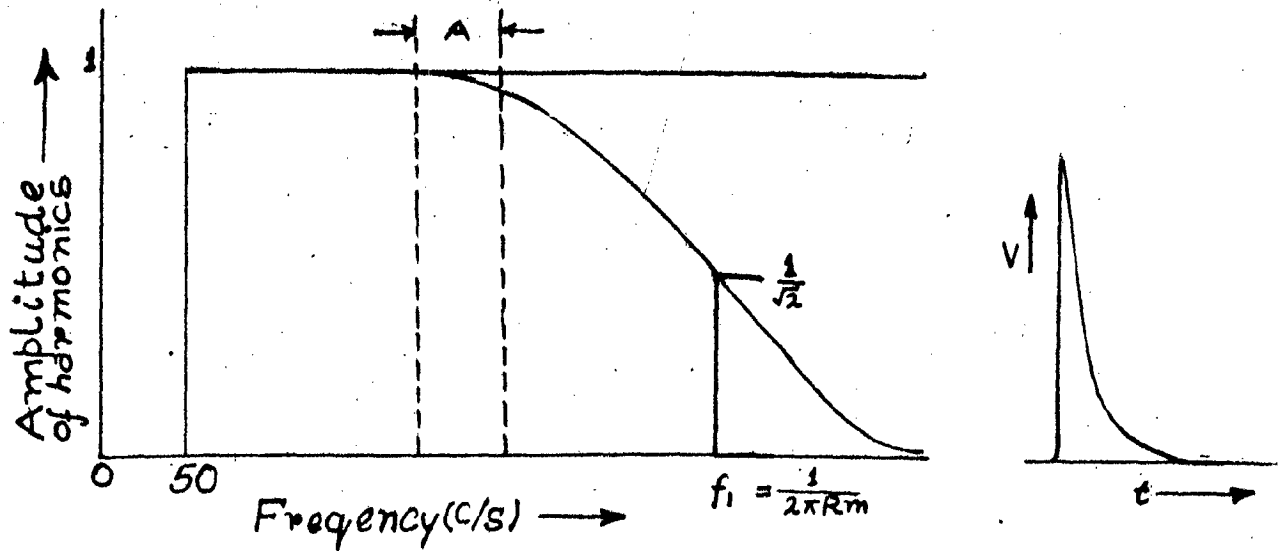
fig. IV.— Frequency spectrum of unidirectional impulses
(RC circuit)
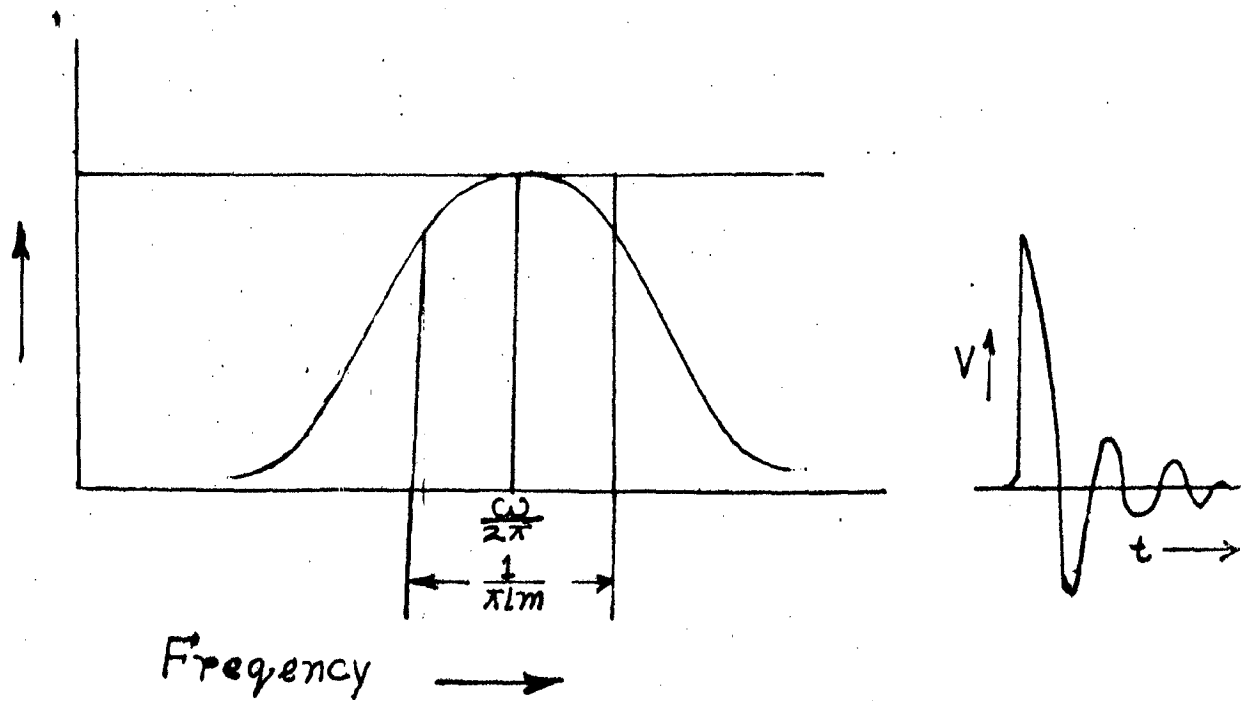
Amplitude of harmonics

$f_1 = \frac{1}{2\pi Rm}$

$\frac{1}{\sqrt{2}}$

A

0   50   Frequency(C/s) →

V   t →

fig. V.— Frequency spectrum of oscillatory impulses
(LCR circuit)

$\frac{\omega}{2\pi}$

$\frac{1}{\pi l m}$

Frequency →

V   t →

Observation - The impulses caused by discharges can be
observed in different ways either separate or integrated.

Loudspeaker - Observation of discharge impulses by means of
earphones or a loudspeaker is simple, but no more information
than the presence or absence of discharges and a rough
estimation of their intensity is obtained.

Voltmeter- A better means is formed by the voltmeter, the
reading of which can be recorded. Several types of voltmeters
are in use. However, a voltmeter has its disadvantages, the
principal being that the reading is as much affected by few
large as by many small discharges.

Oscilloscope - One of the best choices is the oscilloscope.
The discharge impulses usually are displayed on a time base
of the same frequency as the applied high voltage. Recurrent
discharges in successive cycles cover each other and a stationary
picture is obtained. With the aid of an oscilloscope the
magnitude of the individual discharges can be measured, this
magnitude being proportional to the height of the impulses
on the screen. From the character of the picture on the screen
it can sometimes be decided if the observed impulses are caused
by disturbances from the mains, by corona discharges at the
high voltage leads, or by discharges in the object under test.

Sometimes triggering of the time base is preferred, i.e.
the time base is started every time a signal appears. The
impulses which **recur** every cycle of 50 c/s sine wave are
superimposed to form one impulse. With this method a better
separation of discharge impulses and unwanted signals may sometimes
be obtained.

With the elements described above different detection circuits can be built up. Three groups of detection methods may be distinguished:

i. The current impulses in the leads of the sample are transformed into voltage impulses, which are amplified and observed. These methods are called straight detection methods.

ii. The impukses are observed as in (i), but special measures are taken in order to reject disturbanøes caused by discharges in the high voltage source, the leads, terminals etc. These methods are called balanced detection methods.

iii. The power which is dissipated by the current impulses is measured. These methods belong to the loss detection methods.

All these systems are characterized by two important qualities, the sensitivity and the resolution. The sensitivity is is defined by the smallest discharge (stated in pico couloms) which can be detected. With electrical methods the sensitivity depends on the capacitance of the object.

If the discharge impulses are observed separately, either with an oscilloscope or with an impulse counter, the resolution of the detection circuit is of interest. By resolution is meant the number of impulses per unit of time which can be separated. The resolution is also defined by the number of impulses which may be distinguished in

one quadrant of the 50 c/s sine wave. If more impulses per
quadrant are present, an indistinct and hazy picture results.

Straight detection Method

The circuit with which optimum sensitivity and repro-
ducible results can be obtained is described here (Fig. VI).
The high voltage source is discharge free. Moreover, a filter is
provided which blocks disturbances from the mains and from
the transformer. The LCR element is placed in series with
a discharge free blocking capacitor K, the sample a is
earthed so that large capacitors can be tested without large
currents running through the LCR detection element. A series of
LCR elements is provided so that optimum sensitivity can
be obtained for a number of capacity ranges. With these
interchangable element and by varying C, the frequency of
oscillation can ι _always be tuned to the midband frequency of
the amplifier. For this midband frequency 500 kc/s is chosen
because of the absence of disturbances from radio transmission
500 kc/s being the centre of a rescue band.

<div align="center">Components (Fig.VI)</div>

Discharge free transformer,

Filter for suppression of disturbances

a : sample earthed	A : Amplifier, bandwidth 10 kc/s
k : discharge free coupling capacitor	B : Oscillograph : the impulses are displayed on an elliptical time base.
LCR: detection impedence which is interchangable for obtaining optimum sensitivity	C : Calibration impulse with which the discharge impulses can be calibrated (pc).

The bandwidth of the amplifier is 10 kc/s which
permits the resolution of 35 impulses per qudrant of the
50 c/s wave. The sensitivity is high, in an object of
1,000 pF a discharge of 0.02 pC may be detected. The
discharge impulses are displayed on an elliptical trace
which is recorded with a repetition frequency of 50 times per
second. The resulting picture is stable and the location
of discharges with respect to the sine of the test voltage
is clearly visible. An important part of the equipment is
the calibration circuit. A calibration impulse of known
charge content is fed into the circuit. This impulse can
be varied and the resulting picture on the screen can
be made as high as that of the observed discharges. In
this way a direct estimation of the discharges, expressed
in pico coulombs is made.

Balanced detection Methods:- One of the main difficulties
when making discharge tests is discharges which do not
occur in the sample but in other parts of the test circuit,
such as in the high voltage source, in the high voltage
leads, in the blocking capacitor, etc. The impulses caused
by these discharges cannot be distinguished from those
of discharges in the test object, so that they disturb
the observation of the wanted discharges. With the straight
detection methods the effect of these external discharges
can partially be suppressed :

(i) A filter may be used.

(ii) If the detection impedence Z is placed in series
with the sample 'a' and k is made large than a, the impulses
of external discharges are decreased in the ratio a/k.

If the external disturbances are not sufficiently
controlled, a balanced system should be used.

H.F.Schering Bridge:

A method which is often applied makes use of the
Schering bridge which usually is present in a high voltage
laboratory. It is in fact a method with a resistance as a
detection element, as shown in Fig. VII. A discharge in
the sample causes an impulse across resistor R. The impulse
is supplied to an oscilloscope via a filter and an amplifier.
A disturbance from outside causes an impulse across the
resistor on either of the bridges. The difference between
these impulses measured between the bridge points is smaller
than the impulses themselved, impulses from the sample,

however are fully recorded. In this way external discharges
and disturbances are reduced, as well as discharges at the
edge electrodes which are characterized by the fact that
they occur in a capacitor between high voltage and earth.
A minimum is adjusted by varying R' and C'.
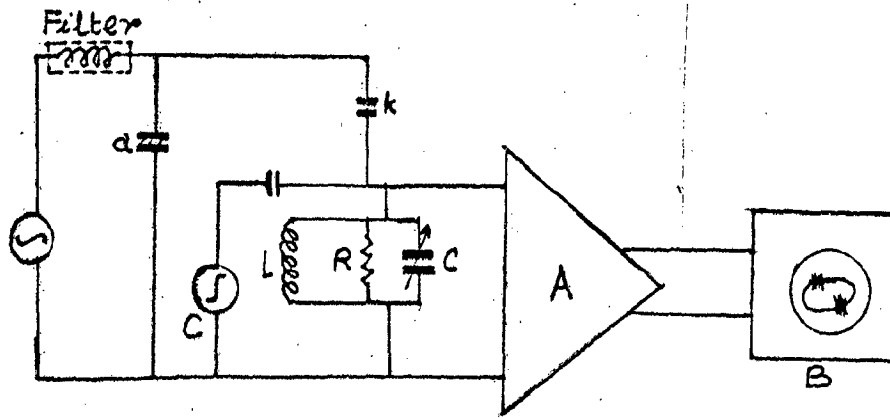
fig: VI :— LCR circuit of Mole. ERA detector
Model I [F1], tuned amplifier.
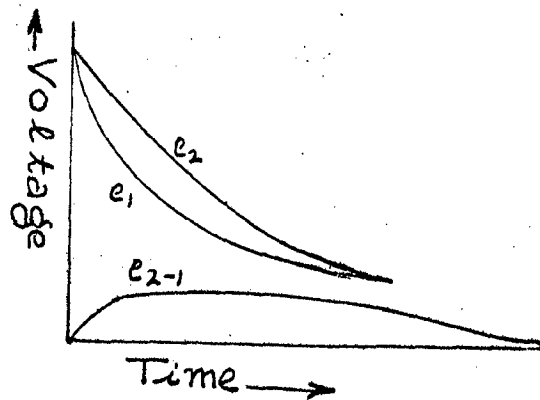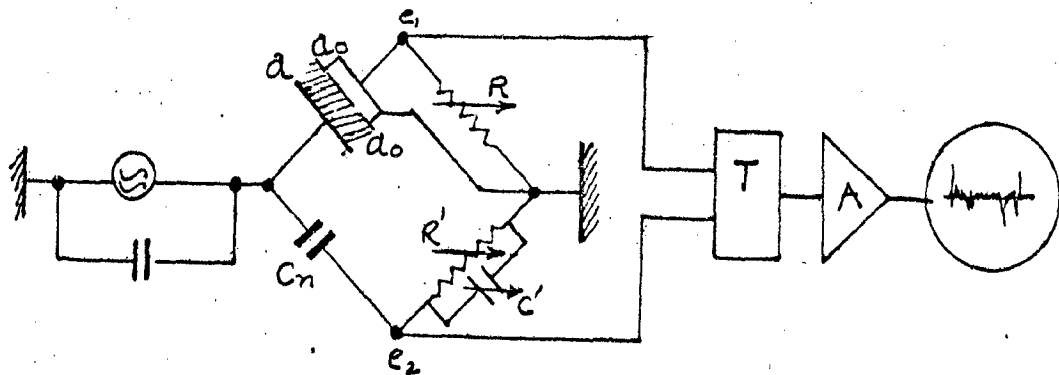
fig. VII :— High frequency Schering bridge circuit as
used for balanced discharge detection

Loss detection methods:

The energy which is dissipated by the current impulses is measured. Measurement of this energy (expressed in the loss-tangent, tan δ) is done by means of a schering bridge. A diagram is made in which tan δ is shown as a function of the voltage U (Fig. VIII). A sudden increase of loss-tangent is attributed to internal discharges, the start of the increase being taken as the inception voltage. But this method is quite insensitive. So we use a double balanced bridge method.

In this method the normal dielectric losses and the losses caused by discharges are separated by means of two different adjustments of the balance. The loss-tangent firstly is measured in normal way, by bringing the bridge to balance with the aid of a vibration galvonometer tan δ_1. Thereafter the galvonometer is replaced by an oscilloscope and the 50 c/s basic frequency is brought to balance : tan δ_2. The part of the loss-tangent which is caused by the discharge is equal to tan δ_1- tan δ_2.
Fig. (IX).
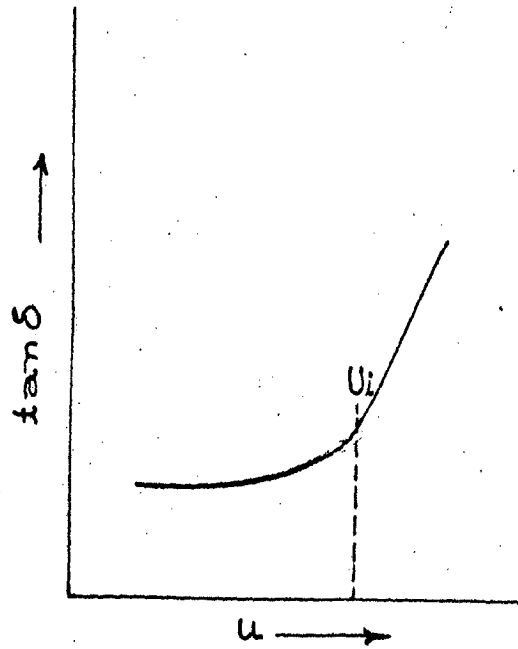
fig. VIII:- Dielectric loss as a function of voltage.
U_i is taken as the inception voltage.
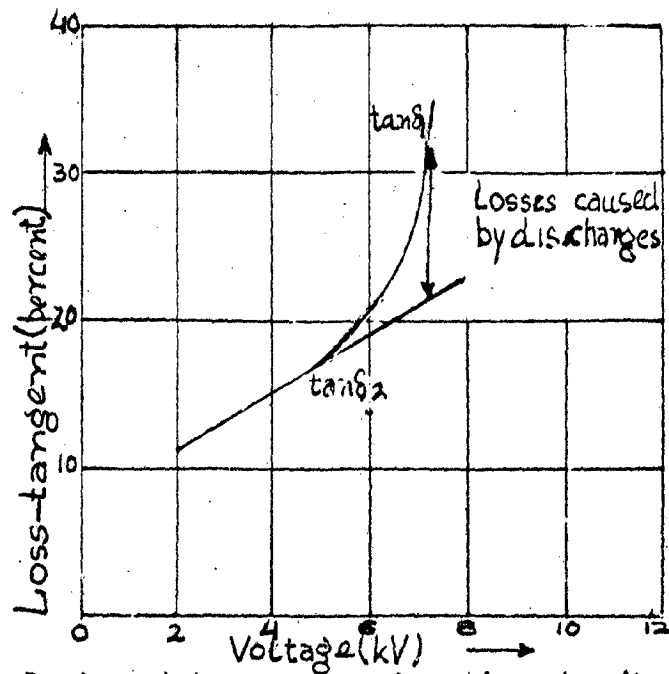
fig. IX:- Dielectric losses as a function of voltage.

```
C          R(5 ), L(5 ), A(5  ),RZ(   ),S(5),G(5)
C          (  I=1,  VIC ='DSK',FILE='AK.D  ')
         ( ,#),( (I),I= ,3),(G(I),I= ,3)
      PT= . 15
         J=1,3
      P I = . 17 26 * (J)
      =( 25/ ELV)+
      (1)= .
        I= , +1
1.    R(I)= . 76+ .52 *FLOAT(I)
         1=1,
2     AL(I)= .7  7.  2/R(I)
      A ( +)= . .
        3  J=1,
      RA(I)= (J)/( . *PT)*1259.7 /(AL(I)-AL(I+1))*ALOG(R(I+1)/R(1))
3     RZ(I)= (J)/(2. *PI)*495 .52/(AL(I)-AL(I+1))*ALOG(R(I+1)/R(1))
          I=
      P I    5 ,R(I),AL(I),RA(I),RZ(I)
5     FOR   (' X, (F19. ,1 X),//)
4     C     U
      P I  *, ( +1)
      S  )= .
      S   = .
           I=1,
      SU 1= S  1+(1/ A(I))
      P  2=   2+(1/ Z(I))
6       I    7 , SU 1
7     F  , (//,J32('*'),//,1 X,'SU  OF CO DUCTANCES=',F17.8,//)
      P T  7 ,SU 2
      SU = .
          J=1,
8     SU =S  +PI*((R(I+ )**2-R(I)**2))*AL(I)
      PRI  9 , SU
0     FOR AT(//,1 X,'SU  OF VOLUME=',E17.8)
1     C  T  UE
      CLOS (U  =1)
      STOP
      E D
```

```
                    R(5 ),  G(5 ),RA(5 ),RZ(5 ),C(5),G(5)
C                   (IT... )  Y,Z1,Z2,Z3
                  =1,DEVICE='D3K',FILE='AK.DAT')
            (*,*),(C(I),I=1,3),(G(I),I=1,3)
       PI=3.1416
       DO   J=1,3
       TLV=.1470261*G(J)
       =(125/TLV)+1
       DO   I=1,N
1      (I)=1 555.7-1 555.7*FLOAT(I-1)/(N+1)
       R(1)=2 .6
       DO  2  I=1,N
2      R(I+1)=R(I)*EXP(6.7 1156-6*AL(I))
       DO 22 I=1,
       =(R(I+1)-2 .6)/ .127
       LA=N+1
22     R(I+1)=LA*0.127+2 .6
       AL(N+1)= . 5
       DO  3  I=1,N
       RA(I)=G(J)/(2. *PI)*125 .7 /(AL(I)-AL(I+1))*ALOG(R(I+1)/R(I))
3      RZ(I)=G(J)/(2. *PI)*485 .52/(AL(I)-AL(I+1))*ALOG(R(I+1)/R(I))
       DO  4  I=1,N
       PRINT  5 ,R(I),AL(I),RA(I),RZ(I)
5      FORMAT(1 X,4(F19.8,1 X),//)
4      CONTINUE
       PRINT *,R(N+1)
       SUM1=
       SUM2=.
       DO  6  I=1,N
       SUM1=SUM1+(1/RA(I))
6      SUM2=SUM2+(1/RZ(I))
       PRINT 7 ,SUM1
7      FORMAT(//,132('*'),//,1 X,'SUM OF CONDUCTANCES=',F17.8,//)
       PRINT 7 ,SUM2
       SUM=.
       DO  8  I=1,N
8      SUM=SUM+PI*((R(I+1)**2-R(I)**2))*AL(I)
       PRINT 9 ,SUM
9      FORMAT(//,1 X,'SUM OF VOLUME=',E17.8)
1      CONTINUE
       CLOSE(UNIT=1)
       STOP
       END
```

```
              X(5  ), W(5  ), RA(5  ), RZ(5  ), G(5), G(5)
                    V  1,25/K3
    OPEN(  ,FILE  =' DSK', FILE=' R. 0 V )
    READ( ,8),(G(I),I=1,3),(R(I),I=1,3)
    PI=3. 116
    DO   I=1,3
    B/U = .76 51* (W)
     =( 5/0 0V)+3
    R(.)=  555.7
    R( )=2  3
    X( )=22.12
              I=1
    AL(I+1)=W(I)-(   W*5.2-(R(I+1)-R(I)))*1055.57/217.62
    P(I+2)= (I+ )* 3 (0.751455-6*AL(I+1))
              I=2
    X=(P(I+1)-2  .5)/  .27
    LA=A+1
    R(I+1)=L *1.127+2  .5
    AL( +1)=
    DO 3  I=1,
    RA(I)=G(J)/(2.  *PI)*1259.7 /(AL(I)-AL(I+1))*ALOG(R(I+1)/R(1))
    RZ(I)=G(I)/(2.  *PI)*485 .32/(AL(I)-AL(I+1))*ALOG(R(I+1)/R(1))
    DO 4  I=1,
    PRI   5 ,R(I),W(I),RA(I),RZ(I)
    F     (X Y, (11.3,1 X),//)
    PRI  *, (  + )
    SU   = .
    S   2=
    D   6  I=1,
    SU  1=SU 1+(1/R (I))
    SU  2=SU 2+(1/RZ(I))
    PRIT 7 , SU 1
    F   T(//, 132('*'),//,1 X,'SUM OF CONDUCTANCES=',F17.8,//)
    PRI  7 , SU 2
    SU  = .
    D    I=1,
    SU =SU +PI*((R(I+1)**2-R(I)**2))*AL(I)
    P  (  ,SU
    F    T(//,1 X,'SUM OF VOLUME=',E17.8)
    C
    C    S (0 I =1)
    S  P
```